U.S.NRC
United States Nuclear Regulatory Commission
Protecting People and the Environment

Technical Letter Report

TLR-RES/DE/REB-2022-09

Technical Support for Component Integrity – Postulated Pipe Rupture Locations:

The Initial Approach, Methodology, Application, and Flaw Stability Assessments for Prototypical Small Diameter Pipe Systems at Normal Operation Plus Service Level-D Limits

Date:

October 2022

Prepared in response to User Need Request NRR-2021-004, by:

E. Kurth-Twombly
Engineering Mechanics Corporation of Columbus

G. Wilkowski
Engineering Mechanics Corporation of Columbus

F. W. Brust
Engineering Mechanics Corporation of Columbus

L. Hill
Engineering Mechanics Corporation of Columbus

NRC Project Manager:

Bruce Lin
Materials Engineer
Reactor Engineering Branch

Division of Engineering
Office of Nuclear Regulatory Research
U.S. Nuclear Regulatory Commission
Washington, DC 20555–0001

DISCLAIMER

This report does not contain or imply legally binding requirements. Nor does this report establish or modify any regulatory guidance or positions of the U.S. Nuclear Regulatory Commission and is not binding on the Commission.

EXECUTIVE SUMMARY

The General Design Criteria (GDC) state that the structures, systems, and components (SSC) important to safety must be designed to accommodate the effects of and to be compatible with the environmental conditions associated with normal operation, maintenance, testing, and postulated accidents. The SSCs must be designed to accommodate the environmental and dynamic effects of postulated breaks as stated in the GDC. Regulatory guidance on postulating pipe ruptures is located in Standard Review Plan (SRP) Section 3.6.2, "Determination of Rupture Locations and Dynamic Effects Associated with the Postulated Rupture of Piping" and its related Branch Technical Position (BTP) 3-4, "Postulated Rupture Locations in Fluid System Piping Inside and Outside Containment" and in BTP 3-3 "Protection Against Postulated Piping Failures in Fluid Systems Inside and Outside Containment".

The current BTP 3-4 outlines criteria for postulating break locations in high energy piping systems based on staff expectations that actual pipe failures occur at high stress or fatigue locations. However, there is no documented technical basis for the criteria outlined in BTP 3-4. The approach is essentially to conduct a conservative S-N based fatigue analysis so that the cumulative usage factor (CUF) is less than or equal to 0.1. For some nuclear power plant (NPP) designs, a CUF acceptance criterion of 0.4 is allowed if the environmentally enhanced S-N curve in the American Society of Mechanical Engineers (ASME) Code is used. With plant life extension evaluations, demonstrating that the CUF remains below 0.1 or 0.4, as appropriate, over the life of the NPP can be quite difficult for the plant operators to meet.

In 10CFR50, Appendix A, GDC 4, allows the use of approved leak-before-break (LBB) analyses to reduce the use of protective hardware, such as pipe whip restraints and jet impingement shielding in piping systems which meet the LBB acceptance criteria. SRP Section 3.6.3, "Leak-Before-Break Evaluation Procedures" provides regulatory guidance for these evaluations. The NRC staff has historically accepted an approved SRP 3.6.3 LBB analysis in lieu of a CUF analysis as per SRP 3.6.2 for demonstrating break preclusion. Traditional LBB evaluations like those in SRP 3.6.3 submittals are generally easy to meet the acceptance criteria for large diameter primary pipe loops but become more difficult to satisfy as the pipe diameter decreases.

The SRP 3.6.3 methodology dates to ~1986, and more recently it has been shown that there are a number of conservative assumptions in that approach. Therefore, in this initial report, rather than performing a traditional SRP 3.6.3 analysis, an advanced LBB evaluation procedure was implemented for a representative 3-inch and 4-inch nominal pipe size (NPS) pipe systems that are employed at a U.S. pressurized water reactor (PWR) and boiling water reactor (BWR), respectively. This report describes the model development and approach, and the results demonstrate that the "critical" crack size of the systems evaluated using an advanced LBB procedure is significantly greater than a traditional LBB evaluation due to eliminating some inherent assumptions in the traditional applied LBB approach. The advanced LBB method used in this evaluation is the Engineering Mechanics Corporation of Columbus (Emc^2) Robust LBB procedure. This procedure uses a finite element model of a piping system which accounts for plasticity from the applied forces and moments, rather than the elastic design stresses used in

the traditional SRP 3.6.3 approach. Additionally, the Robust LBB procedure inserts a crack into the piping system model which more accurately models the crack failure instability, increases the flexibility of the pipe system, and introduces additional local plasticity at the crack section.

New Abaqus finite element (FE) models of the two pipe systems were developed and verified to provide reasonably consistent results with the normal operation stresses from the archived plant piping design report. Once the FE models were verified, the material properties and loading conditions were modified to create a system with broader applicability to other piping systems in the nuclear fleet. The material properties were taken at 550°F for conservatism, and the maximum ASME Code piping design limits for primary, primary plus secondary, and ASME Service Level-D (SL-D) inertial stresses were applied.

The natural frequencies of each of the piping systems were determined in order to define the inertial loading input and direction. Based on the systems' natural frequency, initial applied loading frequencies were chosen for each piping system. Two additional frequencies based on the system natural frequency were applied to the PWR piping system in order to vary the ratio of the seismic anchor motion (SAM) to inertial stresses.

The SAM stresses in a dynamic displacement-time stress analysis are dependent on the difference between the applied and natural frequencies of the pipe system, i.e., if there is an exciting frequency right at the natural frequency to reach the SL-D inertial stress limit, the displacement amplitudes are small and consequently the SAM stresses are small. However, if the excitation frequency is further from the natural frequency, then to reach the same SL-D inertial stresses, the displacement amplitude needs to be much larger, and hence the SAM stresses naturally increase. Consequently, all displacement-time histories were designed to reach the inertial moment limit of SL-D (i.e., $3S_m$), and the resulting SAM stresses were calculated but were much less than the maximum allowable SAM limit in SL-D. The aspect of determining if the SAM stresses were in-phase or out-of-phase with the inertial loading was also examined. The Abaqus FE stress analysis gives the total of the inertial and SAM contributions together. The SAM calculations from the relative end displacements are only to see if the SL-D SAM limits are met.

Using the SAM loading input that reaches the moment corresponding to $3S_m$ inertial loading, an uncracked pipe analysis is performed with the nonlinear stress-strain curve to calculate the reduction of the applied moments compared to the design elastic limits.

A circumferential through-wall crack (TWC) of a small size was then inserted at the high stress location using a cracked-pipe-element (CPE) in Abaqus. The CPE was initially developed and validated in the 1990's and provides computational efficiency to the solution. The crack size was increased until it was at least 75% around the circumference or pipe severance/rupture was reached. The model development and analysis procedure are described in more detail in Section 2.

The findings to date for the two pipe-system geometries involving 3-inch and 4-inch diameter A106B and TP304 stainless steel pipes, showed that when doing the FE time-dependent analyses at the maximum SL-D inertial stress loading, the circumferential cracks were stable for

TWC lengths greater than 75-percent of the circumference. Interestingly, as the crack size is increased, the applied moment decreases with the same inertial loading function. More detailed results are presented in Section 3.

With these same loading conditions, the TWC crack size determined by the traditional SRP 3.6.3 LBB analysis would be too small for the LBB criteria to be met. The reasons for this large difference between SRP 3.6.3 LBB and the advanced LBB prediction of the critical crack sizes is summarized in Section 4.

For potential future efforts, additional sensitivity studies are suggested to explore the limiting pipe-system geometry or boundary conditions that might limit this inherent LBB behavior. Those results would provide guidance to develop screening criteria to identify the type of pipe systems that inherently have LBB behavior without having to conduct the sophisticated LBB analysis as used in this project. For systems that might be borderline, or not pass the new LBB screening criteria, guidance for performing the type of analysis undertaken in this project should be developed. More detail on suggested future work for this project is provided in Section 4.

ACKNOWLEDGEMENTS

The authors benefited from the experience, knowledge, and work of many individuals in performing the analyses in this report. The authors would particularly like to thank Mr. Mark Yoo and Mr. Bruce Lin of the NRC staff for their efforts in leading this project. The authors would also like to thank Mr. Scott Pellet of Southern Nuclear Operating Company and Mr. Mohammed Farooq of Dominion Engineering for their invaluable help in providing information on piping systems and historical software analyses. The authors would like to extend their appreciation to Ms. Renee Li and Mr. Chakrapani Basavaraju of the NRC staff for their comments and review of this work. Finally, the authors would like to thank Mr. Rob Tregoning of the NRC staff for his expertise and knowledge in guiding the technical approach, and for his thoughtful insights and thorough review of the analyses and report.

TABLE OF CONTENTS

LIST OF TABLES

LIST OF FIGURES

ACRONYMS

ASME	American Society of Mechanical Engineers
BPV	Boiler & Pressure Vessel
BTP	Branch Technical Position
BWR	Boiling Water Reactor
CPE	Cracked-Pipe Element
CUF	Cumulative Usage Factor
CVCS	Chemical and Volume Control System
Emc^2	Engineering Mechanics Corporation of Columbus
FE	Finite Element
GDC	General Design Criteria
IPIRG	International Piping Integrity Research Group
LBB	Leak-Before-Break
NPP	Nuclear Power Plant
NPS	Nominal Pipe Size
NRC	Nuclear Regulatory Commission
NSC	Net-Section-Collapse
OD	Outer Diameter
PWR	Pressurized Water Reactor
RCIC	Reactor Core Isolation Cooling
SAM	Seismic Anchor Motion
SAR	Safety Analysis Report
SCC	Stress Corrosion Cracking
SL-D	Service Level D
SMR	Small Modular Reactor
SRP	Standard Review Plan
SSC	Structures, Systems, and Components
TWC	Through-Wall Crack

1 INTRODUCTION

The current BTP 3-4 outlines criteria for postulating break locations in high energy piping systems based on staff presumptions that pipe failures occur at high stress or fatigue locations. However, there is no documented technical basis for the criteria outlined in BTP 3-4. The earlier versions of this approach date back to the 1970s and use methodologies that were conservative and limited due to the lack of operating experience and technological understanding. The approach is essentially to conduct a conservative S-N based fatigue analysis so that the CUF was less than or equal to 0.1. For some NPP designs, a CUF acceptance criterion of 0.4 is allowed if the environmentally enhanced S-N curve in the American Society of Mechanical Engineers (ASME) Code is used. The BTP 3-4 approach also specifies additional reduction factors to the allowable stresses in addition to the Code allowable design limits to demonstrate pipe break preclusion at a location. These factors are intended to account for misalignment and other as-built fabrication departures from the idealized design basis.

In plant life extension evaluations, demonstrating that the CUF remains below 0.1 or 0.4, as appropriate, over the life of the NPP can be quite difficult for the plant operators. Additionally, it is tedious and difficult to document all the actual transients that might have occurred in the prior operating history, and then conduct the stress analyses for each transient. Because of this, conservative assumptions of both the magnitude and frequencies of operational transients is often used in these analyses.

The NRC staff has historically accepted an approved SRP 3.6.3 LBB analysis in lieu of a CUF analysis as per SRP 3.6.2 for demonstrating break preclusion. The GDC establish the minimum requirements for the principal design criteria for a proposed nuclear power facility under the provisions of 10 CFR Part 50 and Part 52. GDC 4 [1] provides the minimum design requirements for environmental and dynamic effects. Under this criterion, it is stated that:

> *The structures, systems and components important to safety shall be designed to accommodate the effects of and to be compatible with the environmental conditions association with normal operation, maintenance, testing, and postulated accidents, including loss-of-coolant accidents. These structures, systems, and components shall be appropriately protected against dynamic effects, including the effects of missiles, pipe whipping, and discharging fluids, that may result from equipment failures and from events and conditions outside the nuclear power unit. However, dynamic effects associated with postulated pipe ruptures in nuclear power units may be excluded from the design basis when analyses reviewed and approved by the Commission demonstrate that the probability of fluid system piping rupture is extremely low under conditions consistent with the design basis for the piping.*

Unless the SSCs qualify for LBB, they must be designed to accommodate the environmental and dynamic effects of postulated breaks as stated. SRP Section 3.6.3 [2] was developed for LBB procedures and gives guidance for performing analysis for plant-specific piping systems demonstrating that the probability of rupture is “extremely low” under the conditions consistent with the design basis and therefore eliminating the necessity of assessing the dynamic effects of a pipe rupture. A conservative deterministic evaluation procedure was initially established to

demonstrate LBB behavior and allow for the removal of pipe-whip restraints and jet-impingement shields should the evaluation show adequate margins with safety factors on leak rate and critical flaw size at transient loading compared to the leakage crack size.

If a piping system does not qualify for LBB, then compliance with GDC-4 must be demonstrated by postulating pipe ruptures and assessing the effects of the hypothesized ruptures on the surrounding equipment. Regulatory guidance on postulating pipe ruptures is located in SRP Section 3.6.2, "Determination of Rupture Locations and Dynamic Effects Associated with the Postulated Rupture of Piping" [3] and its related BTP 3-4, "Postulated Rupture Locations in Fluid System Piping Inside and Outside Containment" [4] and in BTP 3-3 "Protection Against Postulated Piping Failures in Fluid Systems Inside and Outside Containment" [5]. SRP Section 3.6.2 addresses information concerning break and crack location criteria and methods of analysis for evaluating the dynamic effects associated with postulated breaks and cracks in high- and moderate-energy fluid system piping, including "field run" piping inside and outside of containment, which should be provided in the applicant's safety analysis report (SAR). This information is reviewed by the U.S. Nuclear Regulatory Commission (NRC) staff in accordance with the methods of analysis described in SRP 3.6.2 to confirm that there is appropriate protection of SSC's relied upon for safe reactor shutdown or to mitigate the consequences of a postulated pipe rupture.

According to this guidance, breaks must be postulated in Class 1 piping in high-energy fluid systems that do not penetrate containment at the following locations:

1. Terminal ends,
2. Intermediate locations where ASME Code, Section III, Subarticle NB-3653 stress equations (10) and either (12) or (13) exceed $2.4S_m$ for Level A and Level B operating conditions, and
3. Locations where the CUF exceeds 0.1 for Level A and Level B operating conditions.

These current guidelines are conservative and are meant to identify limiting piping locations that experience higher relative stress and fatigue than the remainder of the piping. In addition, the more conservative stress limit (i.e., in comparison with ASME Section III requirements) provides an additional, unquantified stress margin intended to address unforeseen causes such as fabrication and installation errors. The margin adopted on CUF is intended to ensure conservativism to account for unanticipated conditions as well as uncertainties in the quality level of piping systems, uncertainty in vibratory loads, and the lack of explicit consideration of environmental effects which can decrease fatigue life.

A quantitative technical basis for the current stress and CUF acceptance criteria is not documented in SRP Section 3.6.2 nor in BTP 3-4. It has been noted that when environmental effects are included for piping evaluations for plant-life extension, the CUF will likely exceed 0.1. Therefore, a CUF limit of 0.4 has been allowed in some designs when the effect of the environment is considered. However, even this criterion has limited technical basis, and accounting for the current requirements for application of environmental fatigue could lead to an increase in the number of postulated break locations or replacement of pipe systems than the historical CUF < 0.1 criterion. Furthermore, some utility staff members have noted that they had to go through great efforts to try and keep the CUF under 0.1 in more recent plant life extension

evaluations, and in some cases the CUF was higher than 1.0. In the technical sense a CUF of 1.0, in the worst case, should mean that a crack has initiated by fatigue and perhaps grown slightly, but not grown enough for a leak to have occurred. Finally, since the operating experience in the 1970's, it is better understood that there can be other degradation mechanism like stress corrosion cracking (SCC) that can be more prevalent than fatigue, although vibrational fatigue in smaller diameter pipe systems can still be significant.

Most observed pipe failures of pressure boundary (most frequently leaks rather than ruptures) have typically been at unanalyzed locations and caused by degradation mechanisms, which are not addressed in the current guidance but rather are addressed through other programs (e.g., chemistry control, wall thickness monitoring, fatigue monitoring). Further, new reactor designs introduce configurations and connections not previously considered and therefore are not addressed in the current guidance (e.g., bolted connections in Small Modular Reactor (SMR) designs and some nozzle configurations).

Table 4.1-3 of NUREG-1800, Revision 2, "Standard Review Plan for Review of License Renewal Applications for Nuclear Power Plants" [6] (SRP-LR), and Table 4.1-2 of NUREG-2192, "Standard Review Plan for Review of Subsequent License Renewal Applications for Nuclear Power Plants" [7] (SRP-SLR) identify CUF analyses as potential plant-specific time-limited-aging analyses that applicants must address in license renewal applications. Therefore, CUF acceptance criteria must be maintained throughout long-term operation. The longer time period allowed via license renewal will lead to an increase in the number of transient cycles, which in turn is associated with an increase in CUF.

This work is intended to provide a starting point to develop and document a technical basis for developing an alternative BTP 3-4 criteria while still satisfying GDC 4 for current operating reactors as well as taking into consideration new reactor designs. The technical approach aims to provide a method to address the conservative nature of the BTP 3-4 stress and CUF limits and a technical basis for postulating pipe-break locations in piping systems through more rigorous analyses of fluid piping systems, which is applicable to all reactor designs.

2 ANALYSIS APPROACH

2.1 Piping-System Selection

Because BTP 3-4 is generically applicable, any technical basis for updating the current guidance should encompass the range of NPPs currently in operation. Ideally the guidance should also address future nuclear piping system design considerations. Using these ideas, while prioritizing the current operating fleet, a search took place to develop two to three representative piping systems. Several factors were considered in narrowing down the many options available.

As discussed in the introduction, BTP 3-4 gives guidance regarding selecting postulated break locations as outlined in SRP 3.6.2. However, NRC staff have historically approved postulating break locations only when LBB cannot be achieved. Therefore, one of the criteria in choosing piping systems for analysis is that LBB would be difficult to achieve. Based on the experience of the Emc^2 and NRC staff, it is known that the following factors make it more difficult for a piping system to pass LBB:

- Small diameter,
- Low toughness, and
- High inertial loading.

Additionally, the current BTP 3-4 position gives a limit on the CUF of a piping system. Therefore, another consideration in choosing the appropriate piping systems is where meeting the CUF criteria is challenging. In speaking with industry colleagues, Emc^2 was able to obtain pipe-system drawings as well as piping design analysis results for seven different configurations. The configurations analyzed were chosen from this group of systems so that piping design analytical results could be used to verify the accuracy of the finite element results.

Four of the configurations came from a Boiling Water Reactor (BWR) plant, and three came from a Pressurized Water Reactor (PWR) plant. Between the four BWR configurations, two were needlessly complex. The challenge in modeling a complex system is not only the additional time required to model the system and run the analyses, but it is also more difficult to identify the various input contributions to the results. For example, if a system contains many different changes in elevations, and different types of supports, it can potentially require more time or post-processing analysis to determine how much each effect, such as the piping system geometry, the support constraints, or the applied loading contribute to the high stress locations. Between the remaining two BWR configurations, the complexity, pipe diameters and materials were similar, therefore the system with a larger vertical rise was chosen since this would lead to higher dead-weight and probably greater inertial loading. Narrowing down the options for the PWR configurations was similar; one configuration was needlessly complex, and the other two had similar pipe diameters and materials. Therefore, the system with the larger vertical rise was again chosen because of the higher potential for inertial loading. The final choices for the piping systems analyzed are shown in Figure 2-1 for a BWR Reactor Core Isolation Cooling (RCIC) system and Figure 2-2 for a PWR Chemical and Volume Control System (CVCS).

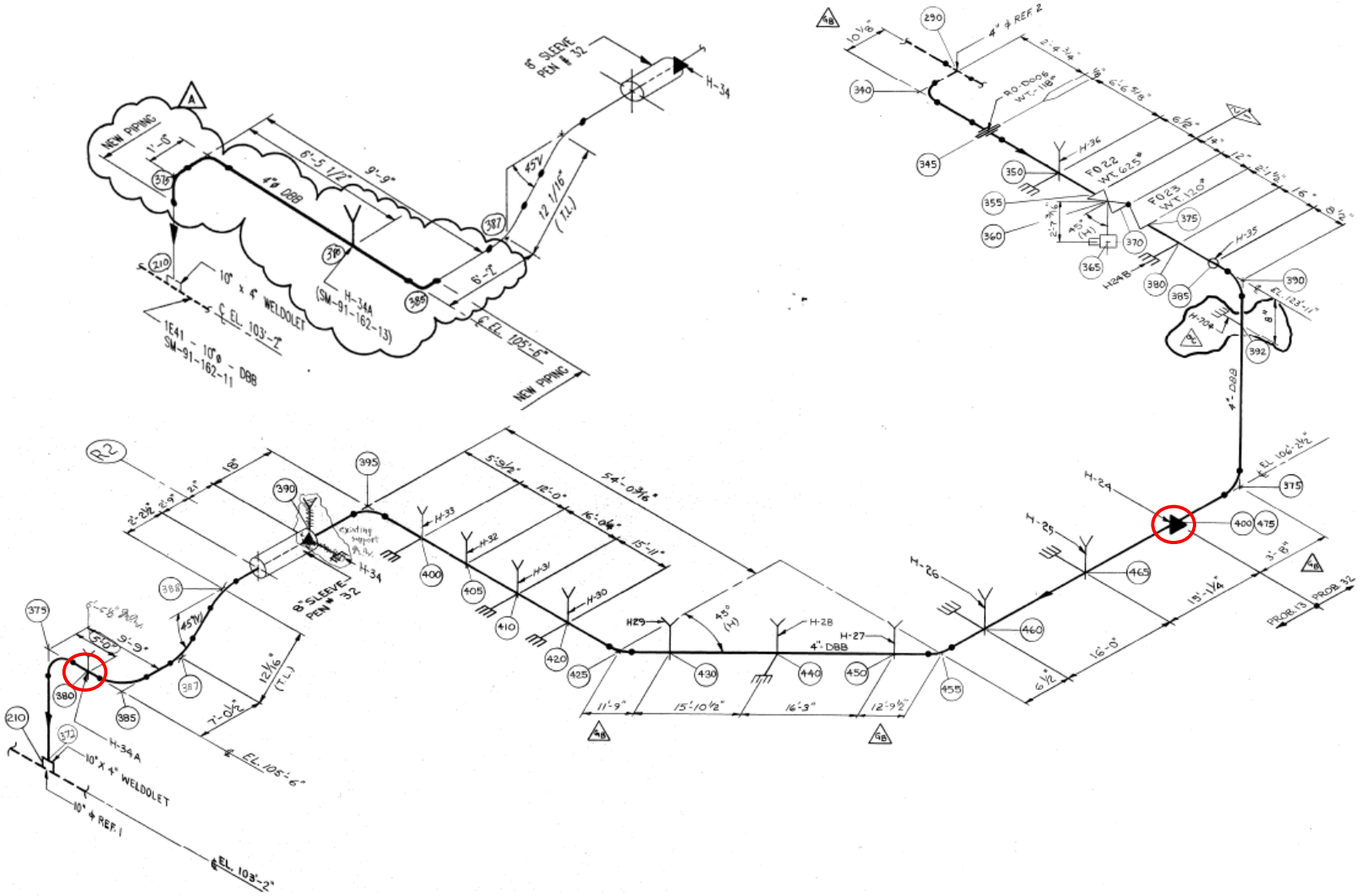

Figure 2-1 BWR representative RCIC system - 4” Test to HPCI test line

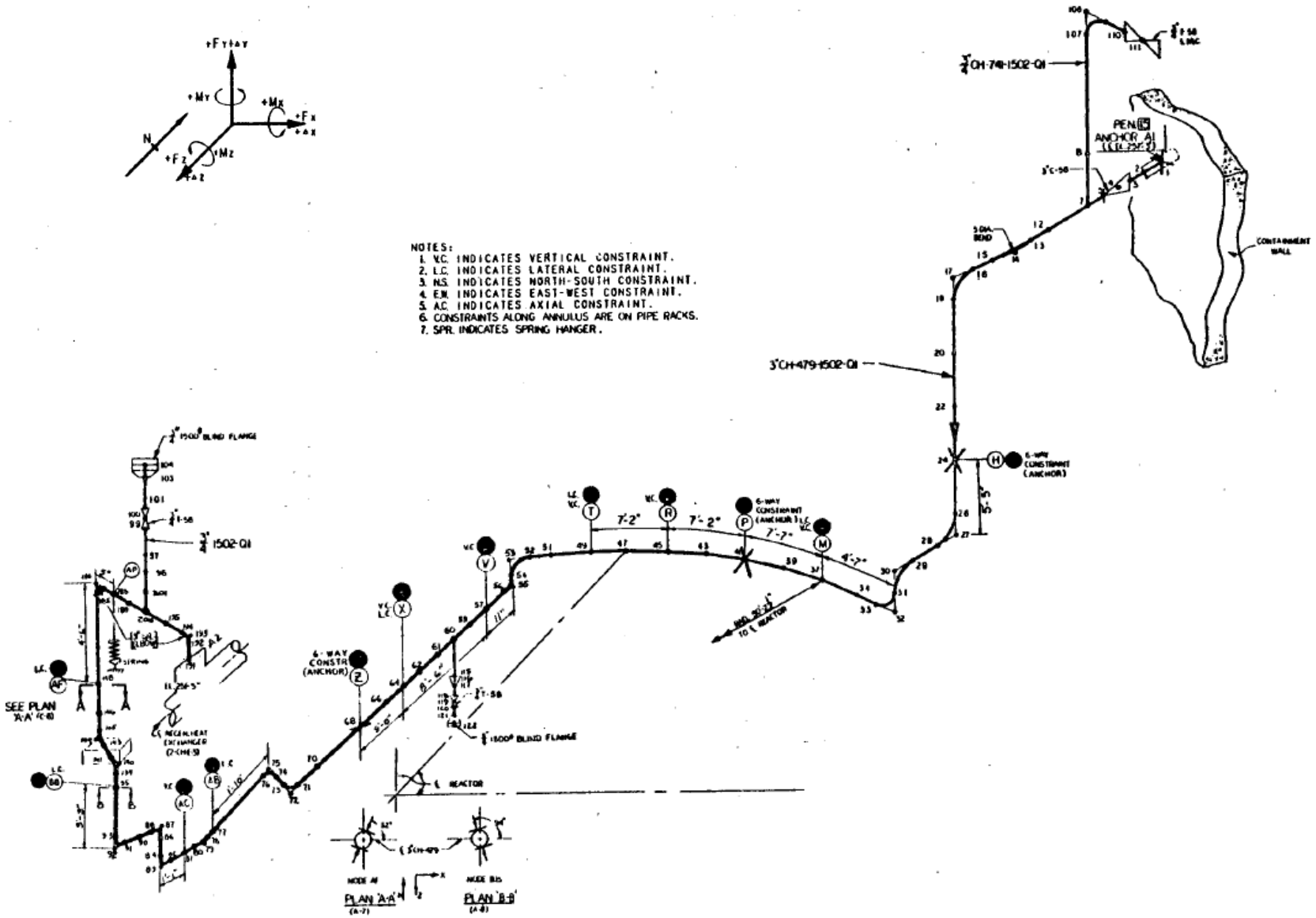

Figure 2-2 PWR representative CVCS – charging line upstream of regenerative heat exchanger

2.2 Analysis Procedure

The analysis procedure described in this section is an advanced LBB evaluation that is used to determine if LBB can be demonstrated in the piping systems modeled. As mentioned in Section 1, pipe ruptures should be postulated at specific locations as per SRP 3.6.2. However, if a piping system qualifies for LBB under SRP 3.6.3, then staff has historically not required break postulation in these systems to satisfy SRP 3.6.2. Therefore, the analysis procedure here will perform a "Robust LBB" analysis on representative piping systems in which pipe ruptures must be addressed under the current guidance. This more detailed "Robust LBB" procedure eliminates several important assumptions that are in SRP 3.6.3, showing that the Robust LBB critical crack is actually much longer than the critical crack determined by the SRP 3.6.3 analysis procedure. Key aspects in the "Robust LBB" procedure are (1) the crack is included in the FE modelling to determine the moments at the crack section, and (2) plasticity from the uncracked pipe system and crack plane can reduce the moments calculated in an uncracked elastic pipe design analysis. The aim of these analyses is to show that LBB criteria is met even in smaller-diameter piping under extreme loading conditions using a non-traditional LBB analysis procedure.

It should be further noted, that even though significant effort was undertaken to obtain realistic piping-system geometries for the FE modelling, additional conservative aspects were included in the analysis. For instance, instead of using the actual plant piping stress analyses, the uncracked-pipe elastic stresses associated with the higher ASME Section III design limits were used. Additionally, the material properties were used at a temperature of 550°F, which is higher than normal operation for these specific lines, but where the strength and toughness of the piping material is lower. This was done to ensure that these analyses were as close as possible to bounding all other piping systems in different types of plants. Therefore, neither of the piping systems analyzed here are for a specific piping system in a nuclear plant but rather were chosen to be representative of a generic small-diameter system with configuration aspects that make it more challenging to demonstrate LBB.

The steps in the analysis procedure are:

1. Develop and verify FE models,
2. Check ASME Code stress limits,
    a. Primary
    b. Primary + Secondary
    c. Determine natural frequency of the system using elastic material properties
    d. SL-D
3. Perform uncracked analysis using ASME SL-D loading from Step 2d to determine the highest stress location and using,
    a. Elastic material properties
    b. Elastic-plastic material properties, and
4. Perform cracked-pipe analysis using elastic-plastic material properties at the high stress location identified in Step 3.

These analysis steps are described in more detail below.

The Step 1 details for the FE model development are discussed in Section 2.3 and the verification details are discussed in Section 3.1.

In Steps 2a and 2b, primary and secondary stress limits were first checked against the original stress analyses of the systems selected to ensure the FE model was reasonably accurate. For the initial evaluations, the temperature difference for thermal expansion stresses was kept at the actual operating plant conditions (95°F for the BWR piping system and 130°F for the PWR piping system), although the material properties were taken at the higher temperature of 550°F. In the future, higher operating temperature could be used to see the effect of the higher thermal expansion stresses, if desired.

Then to be on the conservative side to understand implications for other pipe systems, the SL-D loading used for the inertial loading in Step 2d was the Code maximum allowable stress. Since nonlinear analyses will eventually be conducted, an elastic response-spectrum analysis was not possible. Therefore, a precursor Step 2c is necessary to determine the natural frequency of the piping system in order to develop the initial loading input. The inertial loading was at a single-frequency (either 2 Hz, 3 Hz, or 5 Hz) time-history that ramped up over 2 seconds, had 4 seconds of large amplitude loading at that same selected frequency, and then ramped down again over 2 seconds with that same frequency, see Figure 2-3. These frequencies spanned the first natural frequency of both pipe systems, i.e., when the applied frequency is close to the natural frequency the displacements needed to reach the Code inertial stress limits are small, so the SAM is smaller. At frequencies above or below the natural frequency, the displacements to reach the same Code inertial limit are larger, which yield higher SAM stresses. The SAM displacement amplitude was scaled up or down until the moment from only the inertial loading reached the SL-D limit.

This suggested displacement-time history came from the International Piping Integrity Research Group (IPIRG)-2 program [8] which investigated seismic loading of circumferentially cracked nuclear pipe systems. Based on the results from the experimental pipe-system testing in the IPIRG program, only the large amplitudes with frequencies close to the natural frequency of the pipe loop were important for fracture. Also, 10 to 25 large-amplitude cycles are traditionally used in seismic analyses. In a time-history analysis the total dynamic stress is calculated, i.e., both the SAM and inertial stresses together. However, since the SAM stresses can be out-of-phase with the inertial stresses, the Code allowable inertial and SAM stresses are independent of each other.

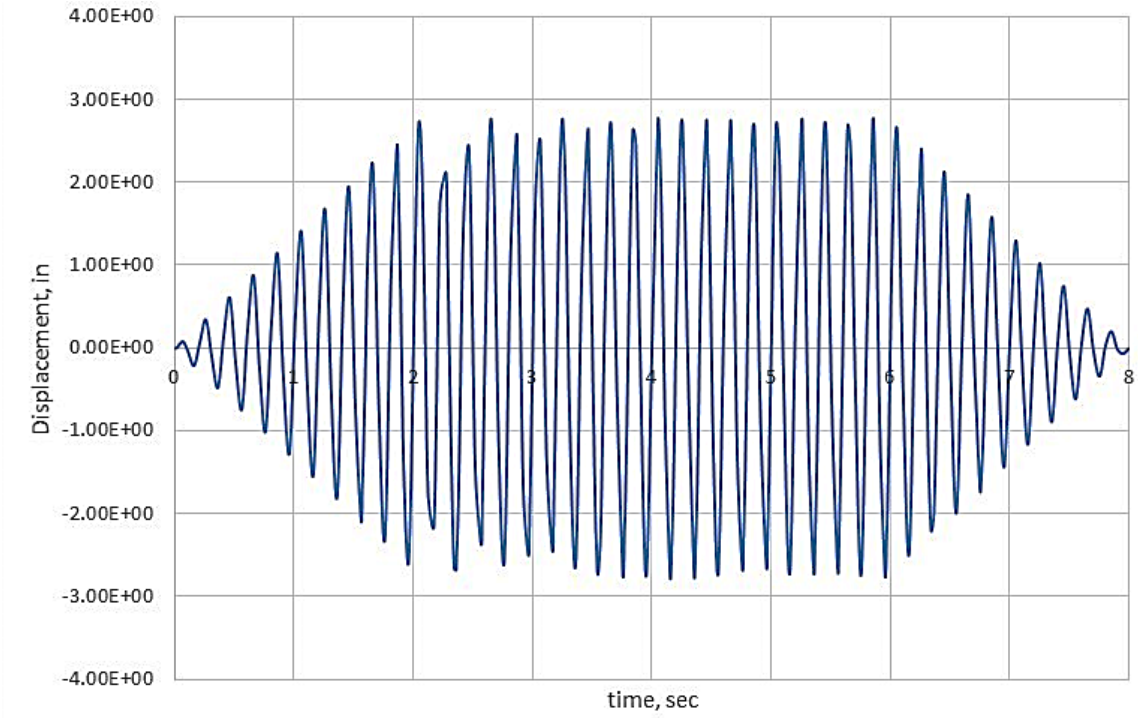

Figure 2-3 Sample of displacement-time history used in dynamic FE analyses to generate the maximum moment in the uncracked elastic pipe analysis for the SL-D inertial limit

The analyses in Step 2 above were elastic uncracked-pipe evaluations more consistent with design analyses per the ASME Boiler & Pressure Vessel (BPV) Code philosophy. To be conservative, only 0.5% damping was applied to the elastic dynamic analyses. In reality, if plasticity is considered as in Step 3b (see below), the effective damping is much greater. The steps to show that the piping systems meet the ASME Section III pipe limits, and the development of the inertial loading input are described in Section 3.2.

In Step 3a, uncracked pipe analyses were first done elastically using the inertial loading determined in Step 2d. Then in Step 3b the pipe system was allowed to undergo elastic-plastic behavior after applying the normal operating plus the same seismic displacement-time histories. The plasticity throughout the pipe system will naturally increase the damping, and plasticity at the crack plane will add additional damping. As one would expect, the elastic-plastic behavior of the piping reduces the applied moments in the pipe system. This step is described in Section 3.3.

Finally in Step 4, a circumferential TWC is inserted at the high-stress location from the elastic analysis. The center of the circumferential flaw needs to be in the principal-bending plane, and oriented with the midplane of the crack coincident with the maximum tensile bending location. The presence of the circumferential TWC affects the natural frequency of the pipe system by making it more flexible, and there may be more plasticity (damping) at the plane of the crack. From past work on circumferential through-wall-cracked piping systems, it has been seen that the applied moments at the crack section can be significantly reduced by the presence of the

circumferential TWC [9, 10]. A key aspect of that behavior is that the dynamic loading does not behave like a load-controlled stress, such that the inertial loading stresses may also be reduced at the crack plane. However, the reason for selecting pipe systems with larger vertical drops and having longer unsupported lengths for greater dead-weight loads was to maximize these stresses at the crack plane. The same loading applied to the uncracked elastic model is applied to the nonlinear cracked model to examine the moment-carrying capacity of the through-wall-cracked pipe system and determine if a large opening area or complete pipe break might occur. The process is repeated with a larger circumferential TWC until either its length is ~80% of the circumference of the pipe or a pipe failure is determined. Section 3.4 describes this step.

2.3 Piping System Finite Element Models

The first step in the analysis procedure consists of the development and verification of the piping-system finite-element models. The finite-element models were developed using the pipe drawings shown in Figure 2-1 and Figure 2-2. All models were created in Abaqus using elbow elements, which allows for the ovalization of the pipe cross section.

Consistent units of force, length, mass, time, and temperature were utilized in all models (see Table 2-1).

Table 2-1 ABAQUS consistent units

Quantity	SI	SI (mm)	US Unit (ft)	US Unit (inch)
Length	m	mm	ft	in
Force	N	N	lbf	lbf
Mass	kg	tonne (10^3 kg)	slug	lbf s^2/in
Time	s	s	s	s
Stress	Pa (N/m^2)	MPa (N/mm^2)	lbf/ft^2	psi (lbf/in^2)
Energy	J	mJ (10^{-3} J)	ft lbf	in lbf
Density	kg/m^3	$tonne/mm^3$	$slug/ft^3$	lbf s^2/in^4

For the FE models in this examination, local coordinate systems are utilized so that the local z-direction is always along the pipe axis, and the y-axis is coincident with the support axis for hanger restraints along that segment.

Verification of the models (shown in Section 3.1), confirmed the boundary-condition definitions where all anchor points are restrained in all degrees of freedom, pinned points are restrained in all translational degrees of freedom, rigid restraints are constrained in the local x- and y-directions, and hanger restraints are restrained in the local y-direction.

More specific information applicable to the two FE models used for this examination are described in more detail in Section 2.3.1 and Section 2.3.2.

2.3.1 BWR RCIC System Model

The BWR pipe drawing for the RCIC system (4” Test to HPCI test line) is shown in Figure 2-1. This system is a nominal pipe size (NPS) 4 Schedule 160 pipe fabricated from A106 carbon steel. The operating temperature is 95°F, the operating pressure is 1,250 psi, and the design pressure is 1,650 psi. The pipe OD is 4.5 inches, and the nominal pipe thickness is 0.438 inches. The finite element model was developed using 2189 nodes and 2188 elbow elements and is shown in Figure 2-4. Elbow elements were used for all pipe sections since they can account for any pipe ovalization during the loading whereas straight pipe beam elements cannot. The insert in Figure 2-4 shows the integration points at each node point for the elbow elements. When the FE analysis is performed, the stress at each of these integration points is calculated. The results for all analyses in this report find the maximum stress of the integration points rather than the average stress of the of those points in order to bound the analysis. This means that at each node point, there are 20 integration points in the cross section and there are 5 cross sections through the pipe thickness, as shown in the insert. The stress at each node point is represented by the maximum stress of those corresponding 100 integration points.

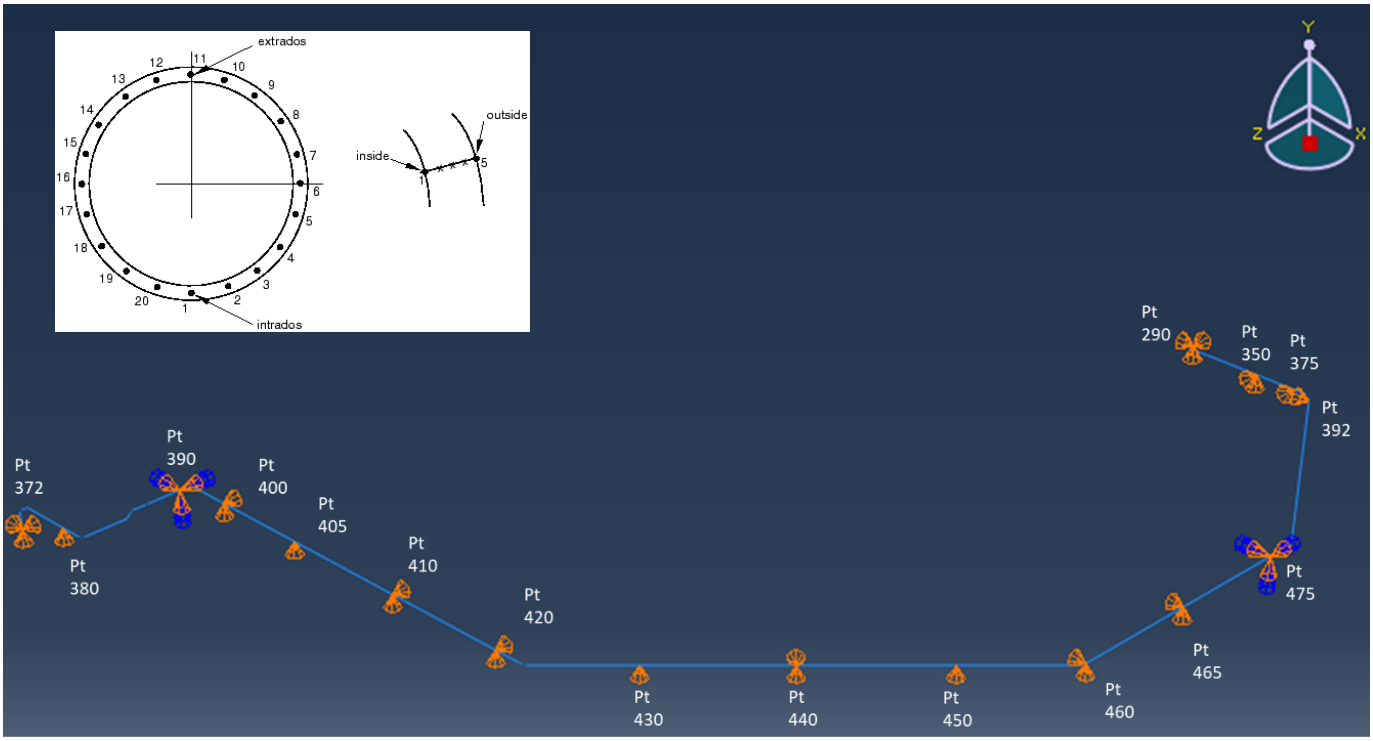

Figure 2-4 BWR RCIC system piping-system finite-element model

The model contains 2 anchor points, at points 390 and 475 in Figure 2-4. There are 13 other support locations, 7 of which are rigid restraints (Points 400, 410, 420, 440, 460, 465, and 350), and 6 hanger supports (Points 380, 405, 430, 450, 392, and 375). The rigid restraints are restrained in the local x- and y-directions but are free to move in the local z-direction, which is along the pipe axis. These are indicated by two orange arrows in Figure 2-4. The hanger supports, indicated by a single orange arrow in Figure 2-4, are restrained only in the y-direction.

The ends of the system are pinned, meaning they are restrained in the translational directions but are free to rotate.

This piping system contains two interesting changes in elevation shown in Figure 2-5. The first is an elevation change of only 8 inches but occurs at a 45-degree angle and is unsupported. The second change in elevation is a 17-foot 8-inch vertical distance which occurs just beyond one of the anchor points. It contains a restraint near the top of the vertical rise. Along the horizontal run at the highest elevation there are 2 valves and a snubber which are represented as inertial mass loads.

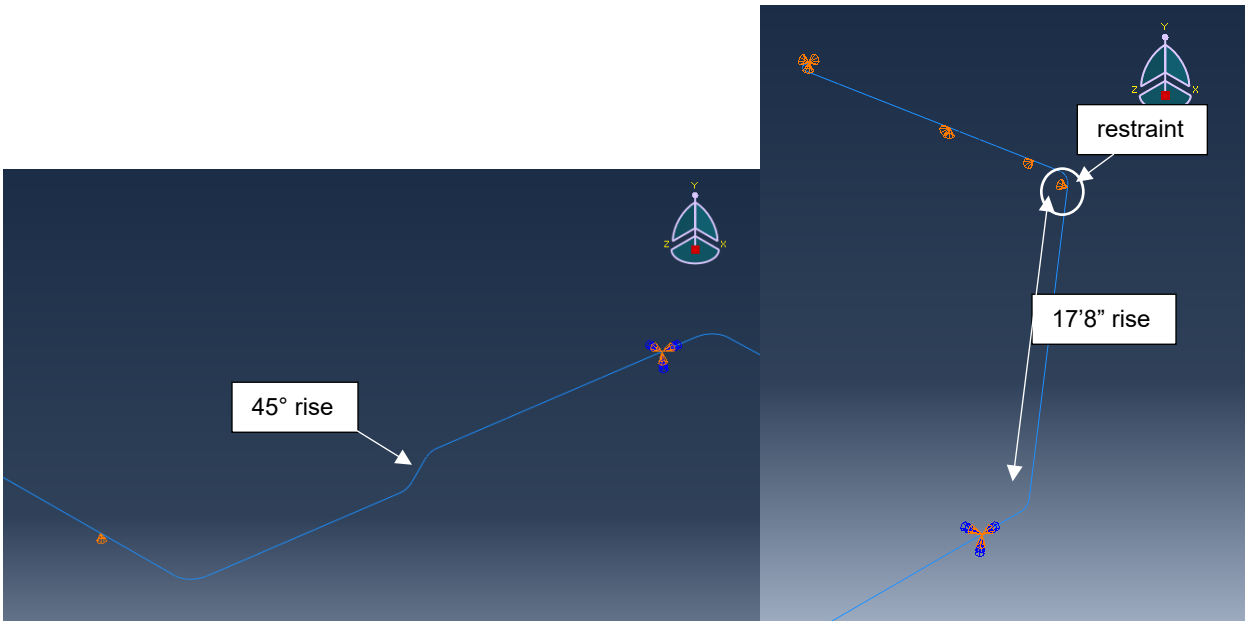

Figure 2-5 Change in elevation details

The A106 material properties used in the analysis are based on data from the pipe fracture (PIFRAC) database, where the original pipe data was generated during the NRC Degraded Piping Program at Battelle [11]. There is much more data for A106B in the database at 550°F than at the operating temperature. For A106B, the yield strength slightly decreases from 95°F to 550°F over that temperature range. The stress-strain curve and J-R curve are shown in Figure 2-6 and Figure 2-7, respectively. Note from past experience, calculation of large crack growth in pipe tests is best done using the J_m-R curve.

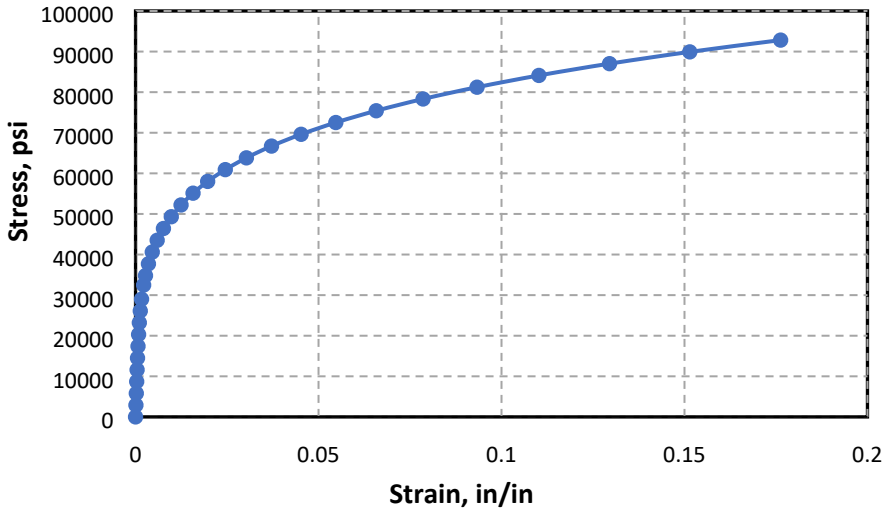

Figure 2-6 A106B lower-bounding stress-strain curve at 550°F (from Pipe #F22)

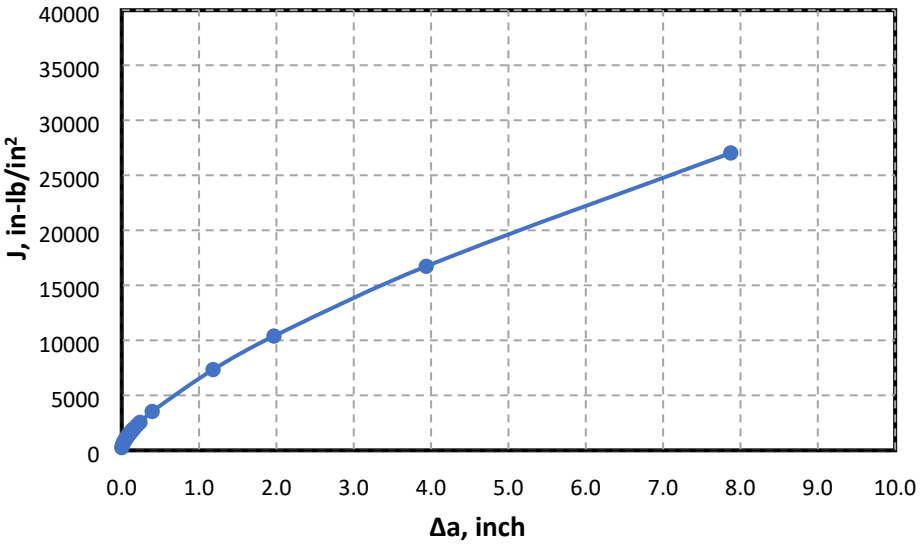

Figure 2-7 A106B J_m-R curve at 550°F (from Pipe #F29)

2.3.2 PWR CVCS Pipe System Model

The PWR CVCS pipe system drawing (charging line upstream of regenerative heat exchanger) is shown in Figure 2-2. This piping system is primarily a NPS 3 Schedule 160, with a small section of NPS ¾ Schedule 160, fabricated from TP316 stainless steel. Given that there is better material property data available for TP304 stainless steel and the difference in strength between TP316 and TP304 is small, it was decided to use TP304 material properties for the analyzed PWR CVCS pipe system. The operating temperature for this model is 130°F, the

maximum operating pressure is 2,375 psi, and the design pressure is 2,500 psi. The pipe OD is 3.5 inches, and the nominal pipe wall thickness that was used in the FE analyses was 0.438 inches. The finite element model is shown in Figure 2-8.

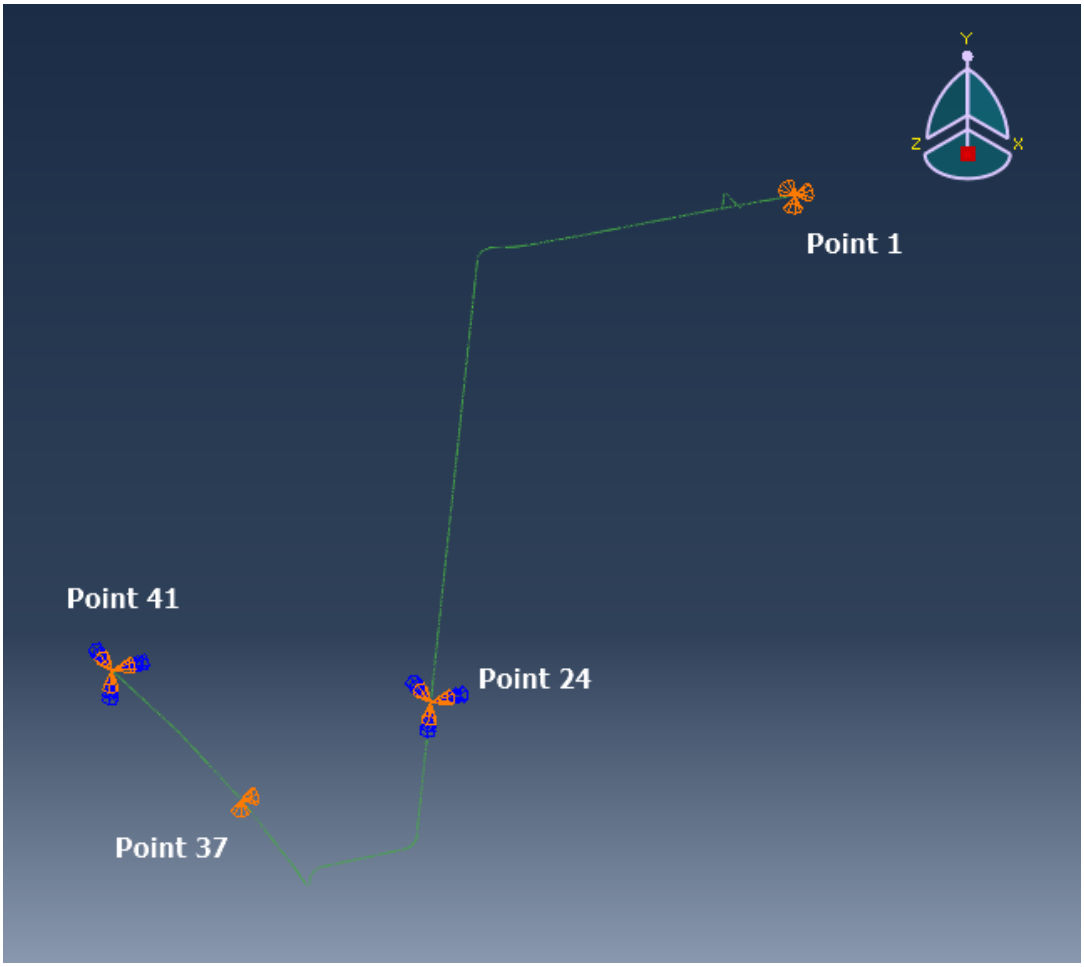

Figure 2-8 PWR CVCS pipe-system finite element model

The Abaqus/Standard model consists of 952 first order ELBOW31 elements. As shown in Figure 2-8, anchor points (i.e., constrained all translational and rotational degrees of freedom) are utilized at Points 24 and 41 and a pinned support (i.e., constrained only translational degrees of freedom) is utilized at Point 1; while Point 37 is a rigid restraint (constrained vertically and laterally in a local coordinate system such that the pipe is allowed to grow axially without constraint). As with the BWR system, elbow elements were used to model the straight pipe sections since they better capture any pipe ovalization than pipe beam elements, and there are 20 integration points along the circumference of the pipe cross section at which the stress is calculated. The maximum stress value of these 20 integrations points is used to determine the high stress locations.

The TP304 material properties used in the analysis are based on data from the PIFRAC database for Pipe #A23 which has a stress-strain curve with the yield strength very close to the

Code minimum at 550°F. The stress-strain curve and J-R curve are shown in Figure 2-9 and Figure 2-10, respectively. In the future, the operating temperature (130°F) could be increased to 550°F to be consistent with the material properties and give higher thermal expansion stresses. Cracks are more stable under thermal expansion stresses which relax with applied displacements when performing nonlinear analyses. Therefore, significant differences are not expected when using the maximum seismic loading if the analyses were conducted at 550°F.

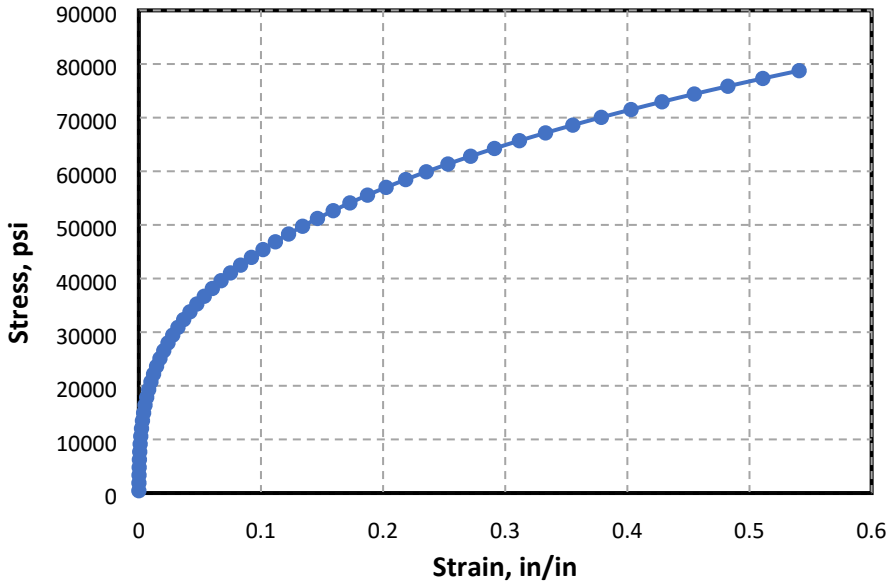

Figure 2-9 TP304 stress-strain curve (from PIFRAC for Pipe #A23)

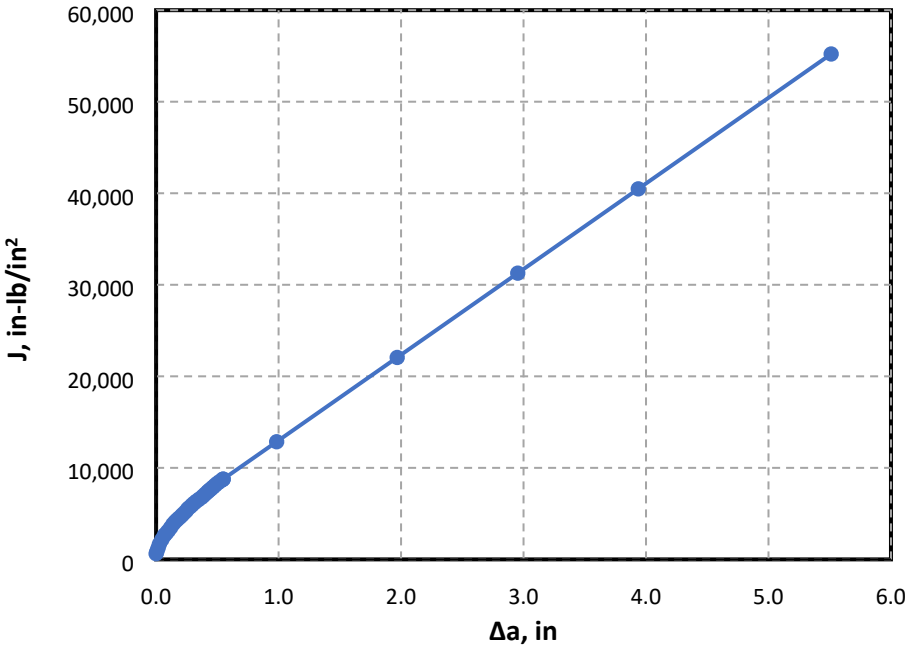

Figure 2-10 TP304 J_m-R curve (from PIFRAC for Pipe #A8W)

3 RESULTS

3.1 Verification

In order to verify that the FE models are accurate, the reaction forces from the FE analysis are compared to prior analytically calculated solutions from old computer codes. In the case of the BWR RCIC system model, results are compared to an analysis performed for the utility in 1982 using the ME101 software program. The PWR CVCS pipe system model, the results are compared to an analysis performed for the utility in 1979 using the NCCODE software program. The boundary conditions of a given finite element model can have a significant effect on the calculated stresses, moments, and forces. This verification ensures that the boundary conditions used in the FE models are interpreted correctly, and that the material and geometry data is consistent.

3.1.1 BWR RCIC System Model

The BWR RCIC system FE model contains piping that was not analyzed as part of the utility's ME101 analysis. Therefore, for purposes of comparing to the ME101 analysis the FE model was truncated. The truncated model is shown in Figure 3-1.

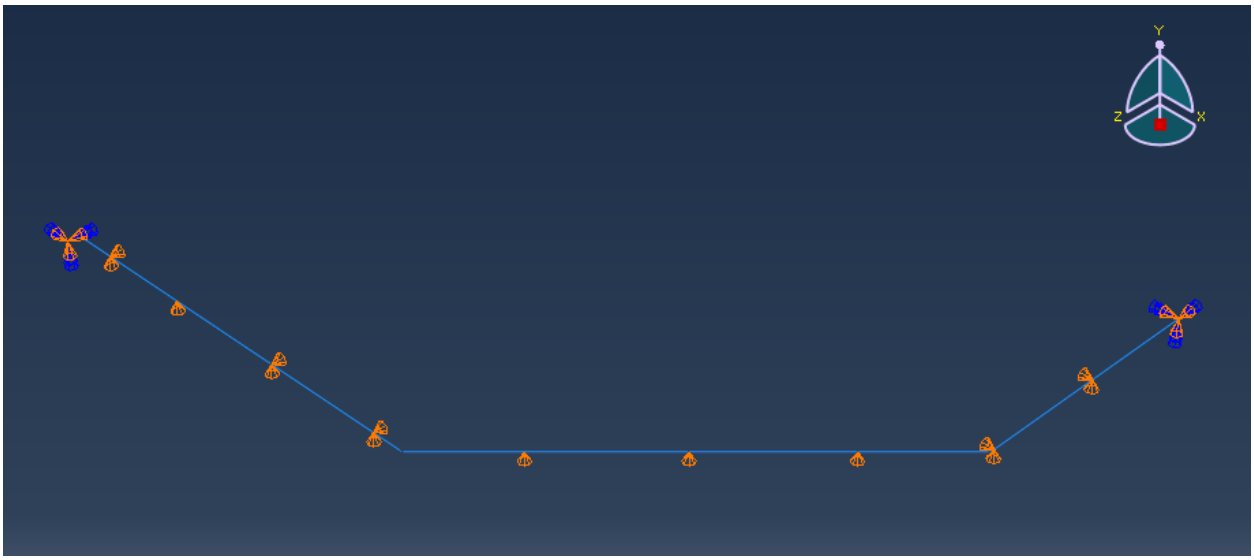

Figure 3-1 Truncated BWR RCIC system FE model

A simple dead-weight analysis was performed and the reaction forces at the supports were compared. The results are shown in Table 3-1.

Table 3-1 Dead-weight reaction forces comparison for the selected BWR RCIC system

Node Label		DW - RF magnitude (lbs)		
ME101	Abaqus	ME101	Abaqus	% error
380	42	439	451.435	**3%**
390	33	265	257.173	**-3%**
400	30	216	216.426	**0%**
405	29	345	345.355	**0%**
410	28	376	378.235	**1%**
420	27	380	379.704	**0%**
430	24	370	369.536	**0%**
440	23	382	381.586	**0%**
450	22	365	364.7	**0%**
460	19	299	299.598	**0%**
465	18	401	400.914	**0%**
475	17	165	165.127	**0%**

As Table 3-1 shows the dead-weight analysis results compare extremely well. The next verification check is for the thermal analysis which consists of a constant temperature rise from room temperature to operating temperature, in this case, 95°F. These results are shown in Table 3-2. Although there are two locations with higher percent error values, these results still match very well, and give confidence that the boundary conditions used to model the piping system supports are accurate.

Table 3-2 Thermal reaction forces comparison for BWR RCIC system

Node Label		Thermal - RF magnitude (lbs)		
ME101	Abaqus	ME101	Abaqus	% error
380	42	3	0.617385	-79%
390	33	1176.102	1205.36	2%
400	30	6	9.73813	62%
405	29	0	0	0%
410	28	224	218.871	-2%
420	27	1275	1259.42	-1%
430	24	0	0	0%
440	23	138.5929	139.304	1%
450	22	0	0	0%
460	19	1131	1118.42	-1%
465	18	18	16.3868	-9%
475	17	1175.011	1162.89	-1%

The comparison in Table 3-2 has two important notes. The ME101 code is still used by the utility for these types of analytical calculations, and it was therefore possible to verify all inputs used in the 1982 analysis. The material density used in the 1982 analysis is different than the density typically used for A106 today. Therefore, to achieve the close match shown in Table 3-2, the Abaqus analysis used the 1982 density value (for the verification exercise only). The other note

is when the analysis was performed on the complete BWR piping system as shown in Figure 2-4 (including modeling the thermal sleeve at node point 390/33) instead of the truncated model shown in Figure 3-1, the percent difference dramatically increased. At node point 390/33, the Abaqus analysis predicts a reaction force with a 236% difference to the ME101 analysis as opposed to 2% when the truncated model is analyzed. Likewise, at node point 475/17 the Abaqus model predicts a reaction force with a 226% difference from the ME101 analysis when the full pipe system is analyzed as opposed to a difference of -1% when the truncated model is analyzed.

The goal of this verification process is to ensure that the boundary conditions and loading are modeled accurately and there are no egregious geometry misinterpretations. The results of the truncated BWR model verify that the geometry is accurately interpretated, the loading is modeled correctly, and modeling the supports as described in Sections 2.3.1 and 2.3.2 is consistent with prior ME101 analyses.

3.1.2 PWR CVCS Pipe System Model

Basic validation checks were performed for dead-weight and uniform temperature rise cases that were provided in the PWR CVCS pipe system pipe stress analysis summary report. Shown below in Table 3-3, the dead-weight summary for the water-filled pipe is an excellent match between the NCCODE model used in the PWR CVCS pipe system design and the current Abaqus model. The one exception is that the PWR CVCS pipe system piping report model extends past Anchor Point 41 which should result in higher reaction force to support the additional piping weight, and at least partially explains the discrepancy in the F_y values at Anchor Point 41.

Table 3-3 PWR CVCS system FE dead-weight comparison to NCCODE

Point No.	Restraint Location/ Description	Calculcated Forces and Moments (Lb and Ft-lb)											
		Fx		Fy		Fz		Mx		My		Mz	
		NCCODE	FEA	NCCODE	FEA	NCCODE	FEA	NCCODE	FEA	NCCODE	FEA	NCCODE	FEA
24	Anchor	-9	-11	-489	-506	19	22	39	64	22	26	-6	-5
37	Lateral & Vertical Rigid	11	11	-159	-154	-28	-25	--	--	--	--	--	--
41	Anchor	-5	-4	-109	-52	-11	11	33	38	-36	-28	-42	-39

The comparison between the Abaqus model and the NCCODE model thermal stresses are given in Table 3-4. There are more significant differences between the two codes in this case. It is likely that the NCCODE is taking into account other factors, such as gaps between supports, but the exact inputs are not clear from the documentation. Such differences are frequently seen when a new Abaqus FE model is compared to an older pipe stress software analysis. The main goal of this verification effort is to ensure that the pipe geometry, loads, and, most importantly, the boundary conditions are being applied correctly. In the analyses for this project, the goal will be to conservatively apply the bounding Code stress values. Modeling supports as rigid boundary conditions without gaps, springs, or other flexibilities is conservative, hence it was decided to model the supports in both the BWR and PWR systems with this conservatism.

Given this goal, the good comparison with the dead-weight loading, and the comparisons shown in the previous section for the BWR system where the inputs are known, the thermal stress comparison for the PWR system was deemed a moot issue.

Table 3-4 PWR CVCS system FE thermal comparison to NCCODE

Point No.	Restraint Location/ Description	Calculcated Forces and Moments (Lb and Ft-lb)											
		Fx		Fy		Fz		Mx		My		Mz	
		NCCODE	FEA	NCCODE	FEA	NCCODE	FEA	NCCODE	FEA	NCCODE	FEA	NCCODE	FEA
24	Anchor	132	159	-15	-91	115	-11	727	75	120	128	970	667
37	Lateral & Vertical Rigid	18	-41	72	-156	97	95	--	--	--	--	--	--
41	Anchor	262	129.2	23	44	130	63	55	35	176	49	-105	-104

3.2 Stress Limits

For break exclusion and LBB to be applicable, the piping design stress limits outlined in ASME BVP Code Section III Division 1, Subsection NB [12] must be met. The piping systems analyzed are pressurized, water-filled pipes, and the welds in these piping systems are assumed to be flush butt-welded girth welds. The BWR small-diameter RCIC system of interest is modeled with A106B carbon steel, and the PWR CVCS pipe is modeled with TP304 stainless steel. The temperature range for these systems is room temperature (70°F) to 550°F. Although the maximum temperature is higher than the normal operating temperature of these systems, it is bounding for high-energy piping systems, and is also conservative from a material strength and toughness viewpoint. Given this information and the pipe geometry, the applicable stress limits can be calculated.

The applicable stress limits for these systems include the primary stress limit, the primary + secondary stress limit, and the SL-D stress limits, which includes the sustained load limit, inertial loading limit, and SAM limit. The following sections show that the primary stress, primary + secondary stress, and the sustained load limits are quite trivial in the actual pipe system. The inertial loading and seismic anchor motion stress limits are more significant, yet both piping systems analyzed meet these requirements. Meeting these requirements is expected since these limits should have been met in the piping system design. However, since slight changes were made to the material properties to genericize the piping systems, it must be confirmed that these stress limits are still met.

3.2.1 Primary Stress Limit

For class 1 piping design limits, Section III Division 1, Subsection NB is used. The primary stress limits are listed per Equation 9 under Article NB-3652, as given below.

$$B_1 \frac{PD_o}{2t} + B_2 \frac{D_o}{2I} M_i \leq 1.5 S_m$$

where

B_1, B_2 = primary stress indices for specific product under investigation
D_o = outside diameter of pipe

I = moment of inertia
M_i = resultant moment due to a combination of Design Mechanical Loads
P = design pressure
S_m = allowable design stress intensity value at Design Temperature
t = nominal wall thickness

For this equation, only the pressure and dead-weight loads are used. For a full-butt-welded girth weld location in a pipe, B_1 = 0.5 and B_2=1.0 according to Table NB-3681(a)-1 (shown below for reference) for flush girth welds.

Table 3-5 ASME Section III Division 1 Table NB-3681(a)-1

Table NB-3681(a)-1
Stress Indices for Use With Equations in NB-3650

	Applicable for $D_o/t \le 100$ for C or K Indices and $D_o/t \le 50$ for B Indices [Note (1)]									
	Internal Pressure [Note (2)]			Moment Loading [Note (2)]			Thermal Loading			
Piping Products and Joints [Note (3)]	B_1	C_1 [Note (4)]	K_1 [Note (4)]	B_2	C_2 [Note (4)]	K_2 [Note (4)]	C_3	C_3'	K_3 [Note (4)]	Notes
Straight pipe, remote from welds or other discontinuities	0.5	1.0	1.0	1.0	1.0	1.0	0.6	0.5	1.0	(5)
Longitudinal butt welds in straight pipe										
(a) flush	0.5	1.0	1.1	1.0	1.0	1.1	1.0	...	1.1	(6)
(b) as-welded $t > 3/16$ in. (5 mm)	0.5	1.1	1.2	1.0	1.2	1.3	1.0	...	1.2	(6)
(c) as-welded $t \le 3/16$ in. (5 mm)	0.5	1.4	2.5	1.0	1.2	1.3	1.0	...	1.2	(6)
Girth butt welds between nominally identical wall thickness items										
(a) flush	0.5	1.0	1.1	1.0	1.0	1.1	0.60	0.50	1.1	(7)
(b) as-welded	0.5	1.0	1.2	1.0	...	1.8	0.60	0.50	1.7	(7)
Girth fillet weld to socket weld, fittings, socket weld valves, slip-on or socket welding flanges	...	...	3.0	...	...	2.0	2.0	1.0	3.0	(8)

Table 3-6 shows the values used for the variables in Equation 9 for the BWR RCIC system and PWR CVCS pipe system models.

Table 3-6 Equation 9 inputs for the piping-system models

Variable	BWR system values	PWR system values
B_1	0.500	0.500
P	1,650 psi	2,500 psi
D_o	4.50 in	3.50 in
t	0.438 in	0.438 in
B_2	1.00	1.00
I	11.66 in^4	5.04 in^4
S_m	18,450 psi	14,900 psi

In this case, the design pressure is used, and the yield stress at 550°F in ASME BPV Section II Code is used [13] . Rearranging Equation 9 gives:

$$M_i \leq \left(1.5S_m - B_1\frac{PD_o}{2t}\right)\left(\frac{2I}{B_2D_o}\right)$$

Therefore, the maximum moment needs to be less than 121,477 in-lb for the BWR RCIC system A106B line and less than 49,984 in-lb for the PWR CVCS pipe system TP304 line in order to meet the Equation 9 stress limits.

For the BWR RCIC system, the maximum moment is calculated to be 10,358 in-lb and for the PWR CVCS system the maximum moment is calculated to be 16,970 in-lb, therefore satisfying the primary stress design limit.

3.2.2 Secondary Stress Limit

The primary plus secondary stress range need to satisfy Equation 10 in Section III Part NB Article NB-3653.1 as given below.

$$\boldsymbol{S_n = C_1\frac{P_oD_o}{2t} + C_2\frac{D_o}{2I}M_i + C_3E_{ab} \times |\alpha_aT_a - \alpha_bT_b| \leq 3S_m}$$

where

C_1, C_2, C_3 = secondary stress indices for specific component under investigation
$E_{a,b}$ = average modulus of elasticity of the two sides of a gross structural discontinuity or material discontinuity at room temperature
M_i = resultant range of moment which occurs when the system goes from one service load set to another
P_o = range of service pressure
$T_a(T_b)$ = range of average temperature on side a(b) of gross structural discontinuity or material discontinuity
$\alpha_a(\alpha_b)$ = coefficient of thermal expansion on side a(b) of gross structural discontinuity or material discontinuity at room temperature

Equation 10 is the combination of the primary and secondary stresses. The C_1, C_2, and C_3 values are in Section III Table NB-3681(a)-1 (see above) for flush girth welds. The C_3 term in all cases considered here goes to 0 since the entire pipe system is at a uniform temperature, and there is no structural or material discontinuity.

Table 3-7 shows the values used for the variables in Equation 10 for the BWR RCIC system and PWR CVCS pipe system models.

Table 3-7 Equation 10 inputs for the piping system models

Variable	BWR system values	PWR system values
C_1	1.00	1.00
P_o	1,250 psi	2,375 psi
D_o	4.50 in	3.50 in
t	0.438 in	0.438 in

C_2	1.00	1.00
I	11.662 in^4	5.04 in^4
S_m	19,225 psi	15,950 psi

In Equation 10, the maximum operating pressure is used, and S_m is the average value of the highest and lowest temperatures (rather than the value at the highest temperature that is used in Equation 9). Since the models are meant to encompass a wide range of applications, a high temperature of 550°F and a low temperature of 70°F are used.

Rearranging Equation 10 gives:

$$M_i \leq \left(3S_m - C_1\frac{P_o D_o}{2t}\right)\left(\frac{2I}{C_2 D_o}\right)$$

Therefore, moment loading, which includes only the thermal-induced bending, needs to be less than 265,655 in-lb for any location along the BWR RCIC system, and 110,479 in-lb for any location along the PWR CVCS pipe system model in order to meet the Equation 10 stress limits.

For the BWR RCIC system, the maximum moment was calculated to be 70,151 in-lb and for the PWR CVCS system the maximum moment was calculated to be 16,594 in-lb, therefore satisfying the primary plus secondary stress design limit.

3.2.3 Sustained-Load Limit from Service Level D

The seismic loading requires the determination of the uncracked pipe elastic limits found in Article NB-3656. The pre-2012 SL-D allowable stress was used for the license application and renewal of most of the current operating fleet systems, but the new SL-D allowable equations allow for much higher stress. Since the more recent equations could be used for future license applications, those limits are used for the piping systems in this analysis.

There are several limits for SL-D loading. The first is the sustained dead-weight load and is given by the following equation:

$$B_2\frac{D_o}{2I}M_W \leq 0.5S_m$$

where

M_W = resultant moment due to weight effects

S_m is at the operating temperature and the moment uses only the dead-weight bending stress. B_2 is again found in Table NB-3681(a)-1 for flush girth welds.

The inputs for this equation for both the BWR RCIC system and PWR CVCS pipe systems are given in Table 3-8.

Table 3-8 Sustained dead-weight load inputs for piping-system models

Variable	BWR system	PWR system
B_2	1.00	1.00
D_o	4.50 inch	3.50 inch
I	11.66 in^4	5.04 in^4
S_m	20,000 psi	17,000 psi

Rearranging the sustained-load dead-weight limit equation gives:

$$M_i \leq 0.5 S_m \left(\frac{2I}{B_2 D_o} \right)$$

Therefore, sustained dead-weight moment needs to be less than 51,831 in-lb for anywhere in the BWR RCIC system, and 24,480 in-lb for anywhere in the PWR CVCS pipe system. For the BWR RCIC system, the Abaqus analysis gives a maximum sustained dead-weight moment of 11,217 in-lb and for the PWR CVCS system the maximum sustained dead-weight moment is 16,882 in-lb.

3.2.3.1 Natural Frequency

The seismic loading history for the finite-element analysis was not given for both piping system cases, and therefore must be developed. Again, to be bounding, the seismic loading is adjusted to go up to the maximum allowable for SL-D loading. The dynamic loading suggested from the IPIRG-2 program on cracked pipe, was to use a single-frequency loading near the natural frequency of the pipe system as a bounding evaluation. The logic being that smaller amplitude loading from frequencies further away from the natural frequency have no contribution of ductile fracture in circumferentially cracked pipes. Hence, the natural frequency of the piping system is used to develop this input. In this process, first the fundamental modes are extracted from the FE model from each of the pipe systems. The first mode for the BWR RCIC system model is at 4.298 Hz and is shown in Figure 3-2.

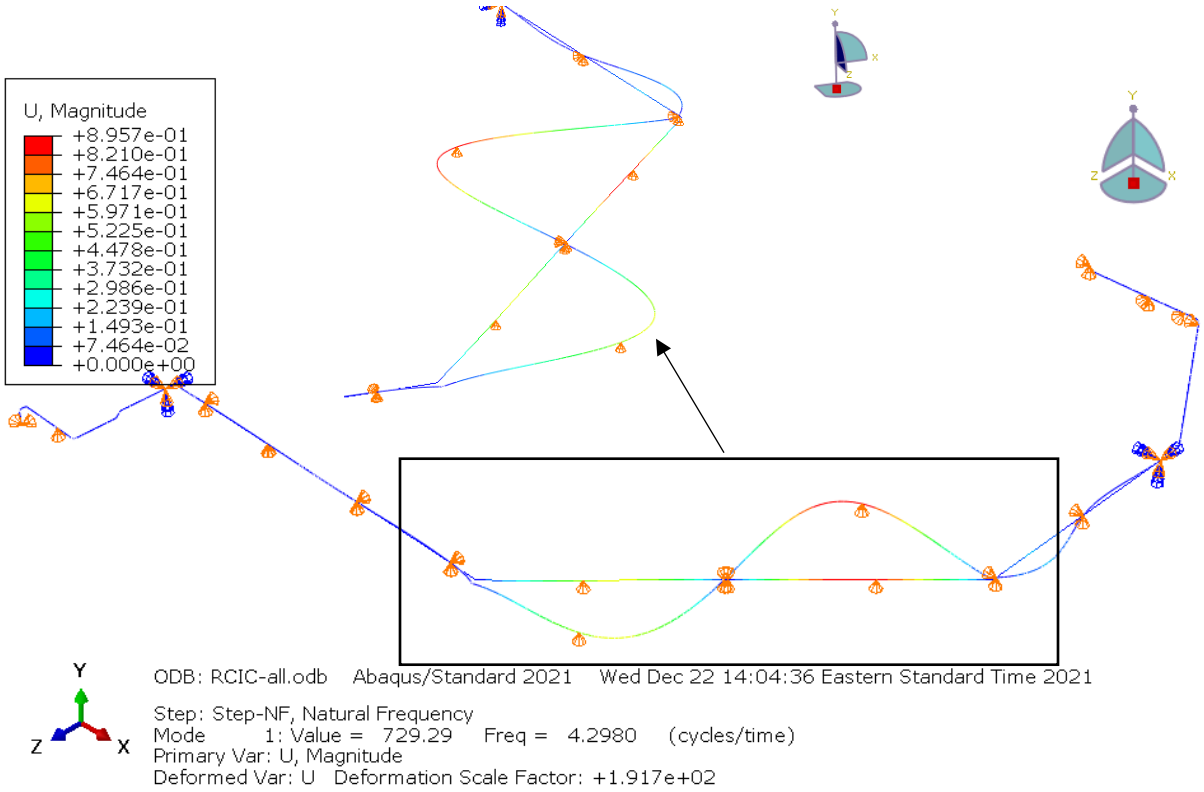

Figure 3-2 First fundamental natural frequency and mode shape for the BWR RCIC system model

The first mode for the PWR CVCS system was found at 2.91 Hz and is shown in Figure 3-3.

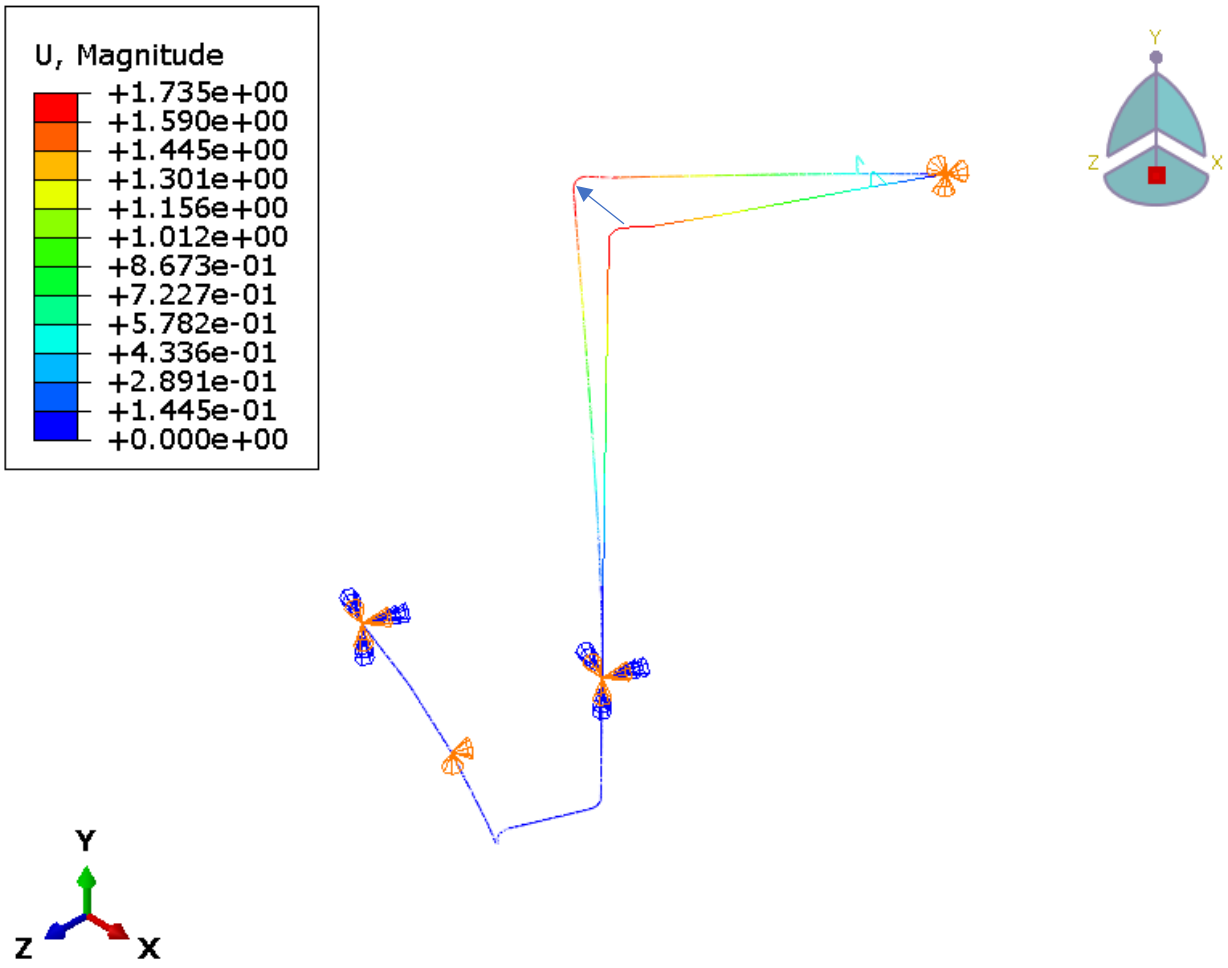

Figure 3-3 First fundamental natural frequency and mode shape for the PWR CVCS system model

The natural frequency for the PWR model is well within the range of common piping systems and in the upper bounding velocity region of the NRC Regulatory Guide 1.60 [14] response-spectrum envelope shown in Figure 3-4 (between points C and D) and the BWR model is near point C.

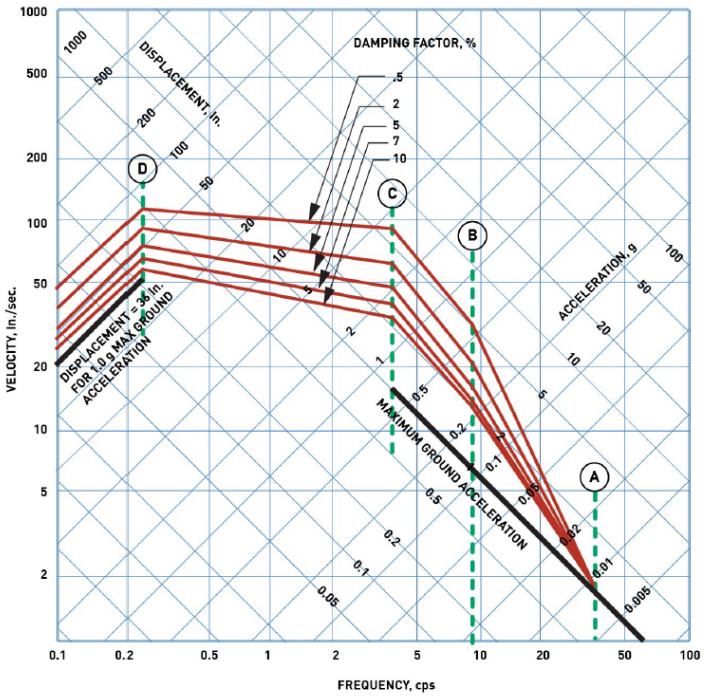

Figure 3-4 NRC Reg Guide 1.60 vertical design response spectra scaled to 1g horizontal ground motion

When conducting traditional design response-spectrum elastic analyses, the inertial contributions are taken from participation factors for each frequency in a bounding response-spectrum curve such as in Figure 3-4 or a site-specific spectrum if known. Frequently, the SAM is taken as a bounding relative displacement of the two anchor points and is treated independently of the inertial motions. In this time-history analysis, the SAM stresses are more precisely calculated, while in past LBB submittals either bounding displacements at anchors were applied or there was no identification of SAM stresses.

Since this approach uses dynamic nonlinear analyses, the SAM stresses are dependent on the applied frequency relative to the pipe-system natural frequency. For example, if the maximum inertial SL-D stress is a target value and the applied frequency is right at the pipe system natural frequency, there is significant dynamic amplification. Therefore, only small amplitude displacements are required. Those small amplitude displacements would give very low SAM values. On the other hand, if the frequency applied is away from the natural frequency, then in order to get to the same SL-D inertial stress limit, larger amplitude displacements are needed due to the smaller dynamic amplifications. These larger amplitudes result in larger SAM stresses. This is illustrated later and is the reason why several different frequencies were selected in the evaluations. Finally, it should be noted that once the circumferential TWC is added in the FE model, the system becomes more flexible, and the natural frequency is lowered. The bigger the crack, the lower the cracked-pipe system natural frequency will be.

3.2.3.2 Inertial Loading

The second SL-D stress limit is for the inertial loads and is given by the following equation:

$$B_1\frac{P_E D_o}{2t} + B_{2'}\frac{D_o}{2I}M_E \leq 3S_m$$

where

$B_{2'}$ = B_2 from table NB-3681(a)-1 with exceptions not applicable for our applications

M_E = the amplitude of the resultant moment due to weight and inertial loading resulting from reversing dynamic loads

P_E = the pressure occurring coincident with the reversing dynamic load

S_m is at the operating temperature, P_E is the pressure at the time of the earthquake, which in all cases in these analyses is the same as the normal operating pressure. According to Table NB-3681(a)-1 B_1=0.5 and $B_{2'}$=B_2=1 for girth welds. In these evaluations, the S_m corresponding to actual plant piping operating temperature rather than 550°F temperature gives a higher (more conservative) limit on the M_E value is used.

The inputs for the SL-D inertial loading equation from ASME Code are shown in Table 3-9 for both the BWR RCIC and PWR CVCS pipe systems. As an added conservatism in the PWR system, the S_m was increased from its value at room temperature (17,000 psi) to the value of the BWR system at room temperature (20,000 psi).

Table 3-9 Inertial loading inputs for piping system models

Variable	BWR system	PWR system
B_1	0.500	0.500
P_E	1,250 psi	2,375 psi
D_o	4.50 inch	3.50 inch
t	0.438 inch	0.438 inch
$B_{2'}$	1.00	1.00
I	11.66 in^4	5.04 in^4
S_m	20,000 psi	20,000 psi

Rearranging this equation gives:

$$M_E \leq \left(3S_m - B_1\frac{P_E D_o}{2t}\right)\left(\frac{2I}{B_2 D_o}\right)$$

Therefore, moment loading needs to be less than 294,346 in-lb for the BWR RCIC system, and 159,136 in-lb for the PWR CVCS pipe system model to meet the inertial moment limit (M_E).

The inertial moment comes from the Abaqus elastic uncracked-pipe stress analysis, where for this effort the pipe system is excited at a specific frequency and amplitude. To achieve inertial loadings, one end of the piping system is fixed, and the other anchor support is excited in the direction that corresponds to the displacements of the piping system at the first natural frequency and with the same amplitude. This is achieved with a displacement-time history in the horizontal X-Z plane as vertical displacements are typically much lower (this was verified to be the case with both piping systems). For the case of the PWR CVCS pipe system, three frequencies that were above, near, and below the system natural frequency were chosen: 2 Hz, 3 Hz, and 5 Hz. The BWR RCIC system was run only at a single frequency of 5 Hz, which is above the system natural frequency of 4.298 Hz but below the 2nd natural frequency of 5.1886 Hz. Once the excitation frequency is chosen, the amplitude is adjusted until the M_E limit is reached. To achieve this within Abaqus, a DISP displacement user subroutine was utilized.

Additionally, since all systems contain some degree of damping, this was accounted for by using 0.5% mass-proportional Rayleigh damping in all analyses, which is a minimum for elastic response of just the piping with no plasticity and damping from hangers/supports. In subsequent time-history analyses, the natural plasticity in the uncracked pipe and in the crack plane both add to the damping as in realistic piping system.

The corresponding amplitude for each of the driving frequencies (2 Hz, 3 Hz, and 5 Hz) that were applied to the PWR CVCS system model is 8.0 inches, 1.1 inches, and 8.75 inches, respectively. Again, this shows that near the natural frequency not much displacement is needed to get to the inertial moment limit. The BWR RCIC system model had an amplitude of 6.6 inches corresponding to the driving frequency of 5 Hz. These displacements correspond to the maximum allowable stress ($3S_m$) in the SL-D stress limit equation at each driving frequency.

The Abaqus analysis gives a corresponding maximum moment for the PWR CVCS pipe system of 142,800 in-lb at 2 Hz, 144,900 in-lb at 3 Hz, and 146,900 in-lb at 5 Hz. For the BWR RCIC system the Abaqus analysis gives a maximum moment of 178,181 in-lb. Therefore, both systems were below the inertial loading limit in the current ASME Section III – Subsection NB for SL-D events.

3.2.3.3 Seismic Anchor Motion

The third SL-D stress limit is in regard to seismic anchor motion and is given by the following set of equations:

$$C_2 \frac{M_{AM} D_o}{2I} < 6.0 S_m$$

$$\frac{F_{AM}}{A_M} < S_m$$

S_m is at the operating temperature, and C_2=1.0 according to Table NB-3681(a)-1 for girth welds. F_{AM} is the longitudinal force resulting from the anchor motions due to earthquake, A_M is the pipe

cross-sectional area, and M_{AM} is the moment resulting from anchor force motions due to earthquake [12].

The inputs for the SL-D SAM limit equations are shown in Table 3-10 for both the BWR RCIC system and PWR CVCS pipe system FE models.

Table 3-10 Seismic anchor motion inputs for both piping-system FE models

Variable	BWR system	PWR system
D_o	4.5 in	3.5 in
C_2	1.0	1.0
I	11.662 in^4	5.04 in^4
S_m	20,000 psi	20,000 psi
A_M	5.594 in^2	4.213 in^2

Rearranging these equations gives:

$$M_{AM} < 6S_m\left(\frac{2I}{C_2 D_o}\right) \qquad \text{and} \qquad F_{AM} < A_M S_m$$

Therefore, the SAM moment loading needs to be less than 621,973 in-lb for the BWR RCIC system, and below 345,600 in-lb for the PWR CVCS pipe system model in order to meet the SAM moment limit. The anchor motion force should be below 111,880 lb for the BWR RCIC system, and below 84,260 lb for the PWR CVCS pipe system.

To determine the amount that the end of the piping system should be displaced, the maximum displacement need to reach the inertial loading limit is used. This is because when the time-history analysis for the inertial loading analysis is performed, the movement at the one anchor point to satisfy the inertial loading is actually applying SAM at the same time. If the loading is right at the natural frequency, then the displacements are small, and the SAM is close to zero. If the applied frequency is far from the natural frequency, then the displacements are large, and the SAM is higher. This is verified by the relationship between the driving frequencies and amplitudes for the PWR CVCS system reported in the previous section and shown in Table 3-11 for convenience. Near the natural frequency of 2.91 Hz the amplitude is small in comparison to the other two frequencies, which are further from the natural frequency.

Table 3-11 Frequency and amplitude relationship for PWR CVCS pipe system

	Values for reaching SL-D inertial stress limits		
Freq (Hz)	**2.00**	**3.00**	**5.00**
Amplitude (inch)	**8.00**	**1.10**	**8.75**

Therefore, to determine if the SL-D SAM limit is satisfied, the maximum displacement needed to reach the inertial loading limits (i.e., 8.75” in Table 3-11) is used as a static displacement in the Abaqus analysis. This static displacement is applied in conjunction with the inertial dynamic

loading as discussed in Section 3.2.3.2. Since the SL-D SAM limit is higher than the SL-D inertial loading limit, and the SAM and inertial loading are applied through the same displacement loading, then by default the SAM limit is met when the inertial loading limit is met.

3.3 Uncracked Pipe Analysis

To determine the highest stress location in the piping system, an uncracked analysis was performed. The analysis was run with primary and SL-D loading as described above. This uncracked pipe analysis was first run using only elastic material properties, and then again with nonlinear properties.

The PWR CVCS system model uses three driving frequencies, 2 Hz, 3 Hz, and 5 Hz in three separate FE runs, but the BWR RCIC system model uses only a 5 Hz driving frequency as described in Section 3.2.3.2. The high-stress location under a 5 Hz driving frequency for the BWR RCIC system model is determined to be the elbow location about mid-way between the two anchor points. Figure 3-5 shows this location circled in black and the anchor points circled in red.

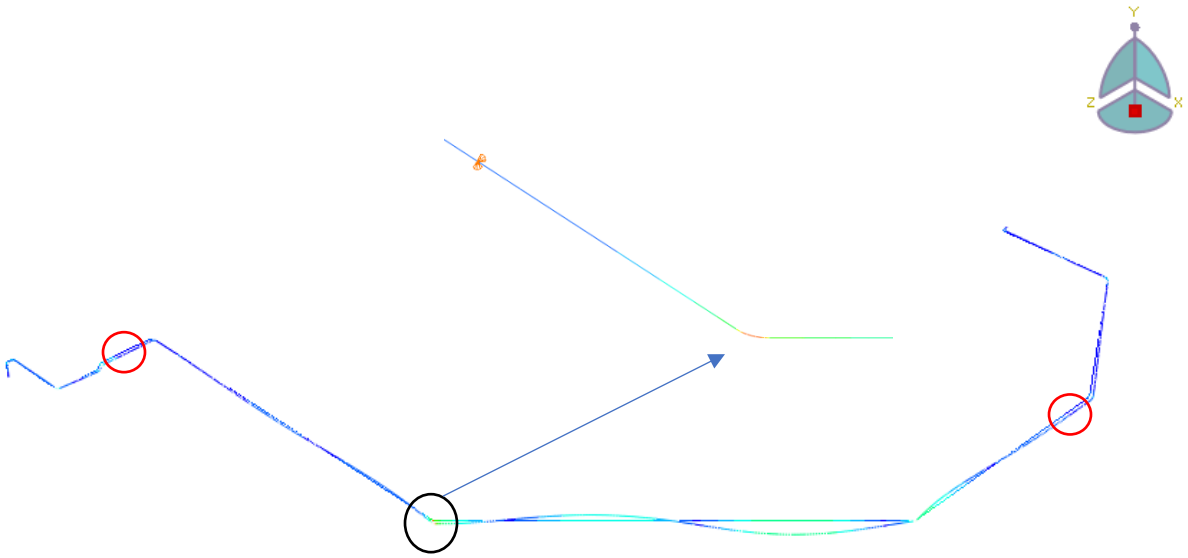

Figure 3-5 High stress location for the BWR RCIC system model (circled in black)

The high stress location for the PWR CVCS pipe system model is along the vertical rise section as shown in Figure 3-6. This is the high stress location for all applied frequencies.

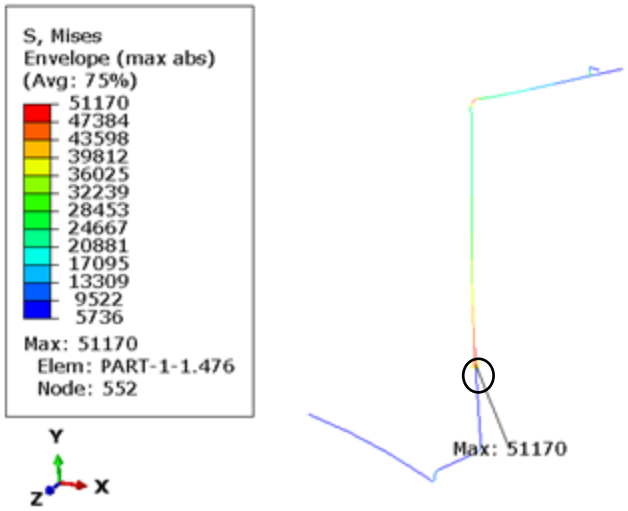

Figure 3-6 High stress location for the PWR CVCS system model (circled in black)

3.4 Cracked-Pipe Analysis

Once the high stress location is determined from the uncracked pipe analysis, the next step is to insert a crack into the pipe at this location with the circumferential TWC centered on the principal direction bending plane using a "cracked-pipe element" (CPE). Initially a small crack is inserted in the pipe at this location, and the analysis is run with normal operating plus SL-D loading. The change in moment is examined, and if the maximum rotation has not been reached then a larger crack is inserted at the same location. This process is repeated until either the crack has reached ~80% of the circumference of the pipe or the maximum rotation of the CPE is reached. The maximum rotation is the condition where a complete severance of the pipe (rupture) occurs, whereas a maximum moment would traditionally be used in an SRP 3.6.3 type of LBB analysis (i.e., assuming the pipe breaks at maximum moment with all loading being assumed to be load-controlled).

The CPE element approach was first developed in the IPIRG program [15]. It represents the local strength of the cracked pipe in terms of moment and rotation. The local moment-rotation curve is nonlinear and comes from the LBB.ENG2 J-estimation scheme in the NRCPIPE code which was developed and validated in many past NRC pipe fracture programs. When using Abaqus, the CPE is created using a connector element that is inserted between two other elements at coincident node points. The input to the LBB.ENG2 J-estimation scheme includes the material stress-strain curve and the J-R curve for the material fracture resistance as well as the pipe and crack geometries. The following section gives further details on the CPE methodology.

3.4.1 Background of the Cracked-Pipe Element (CPE)

The process of growing a circumferential surface crack and/or a TWC in a piping system can go through the experience of starting with surface-crack growth through the thickness and subsequently transitioning to a circumferential TWC, and finally from a TWC to a complete pipe

break. For this report, the concern is for circumferential TWC growth. The crack-opening area is related to the rotation of the cracked pipe, and the transformation from rotation to opening area can also be determined.

Figure 3-7(a) schematically shows the moment-rotation curve for a pipe with a circumferential surface-crack developing to a circumferential TWC. The crack experiences elastic loading, plastic deformation, reaches the maximum load capacity, and then grows through the thickness. Figure 3-7(b) is the moment-rotation curve for a pipe with a circumferential TWC crack from loading until break and shows that the load capacity decreases from crack growth after reaching the maximum point. The full process from a surface crack to TWC and break is schematically presented in Figure 3-7(c). During the transition from a circumferential surface crack to a circumferential TWC, there is often a sudden decrease in load depending on the surface crack length. By subtracting the elastic and plastic rotations of the uncracked pipe from the total rotation including the crack, the rotation due solely to the crack can be determined. It is the moment versus rotation *due to the crack* that is calculated by various fracture mechanics analyses [16] and then implemented into the "cracked-pipe element" method.

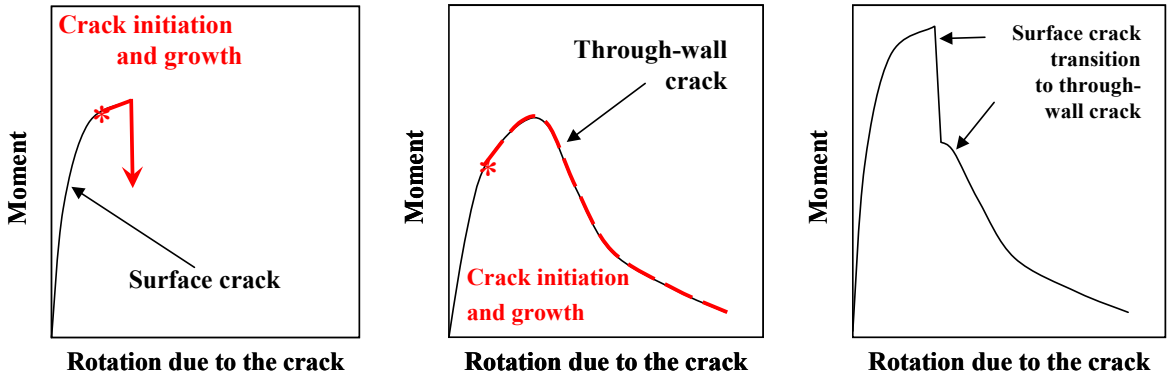

Figure 3-7 Moment versus rotation-due-to-the-crack curves from initial loading to full break of a pipe with a circumferential crack

During the early 1990's, multiple springs, sliders, and pin elements had to be used in ANSYS to simulate the whole process in the IPIRG program as shown in Figure 3-8. However, in recent work [9], a new type of Abaqus element, a "connector element", was used to simulate the elastic, plastic, and post maximum load (damage) behavior of a crack as shown in Figure 3-9.

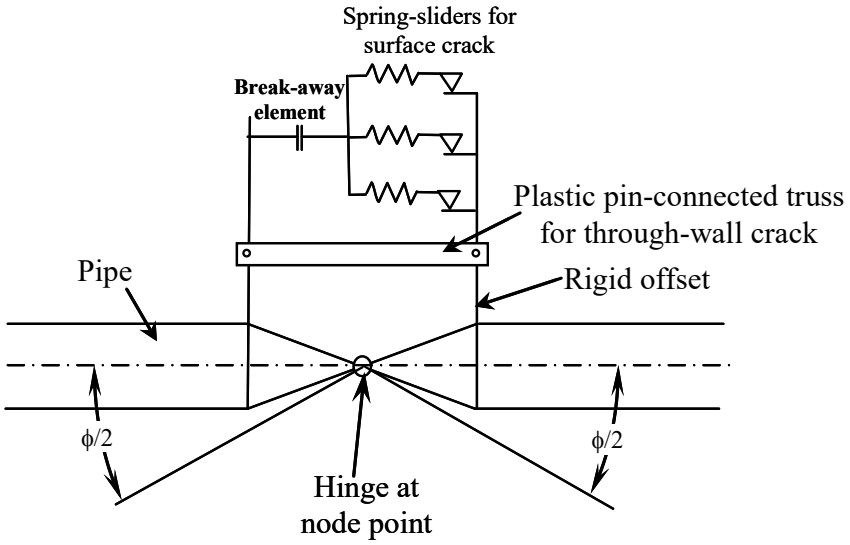

Figure 3-8 Schematic of types of elements used in ANSYS in past to model the moment versus rotation-due-to-the-crack curves from initial loading to full break of a pipe with a circumferential crack

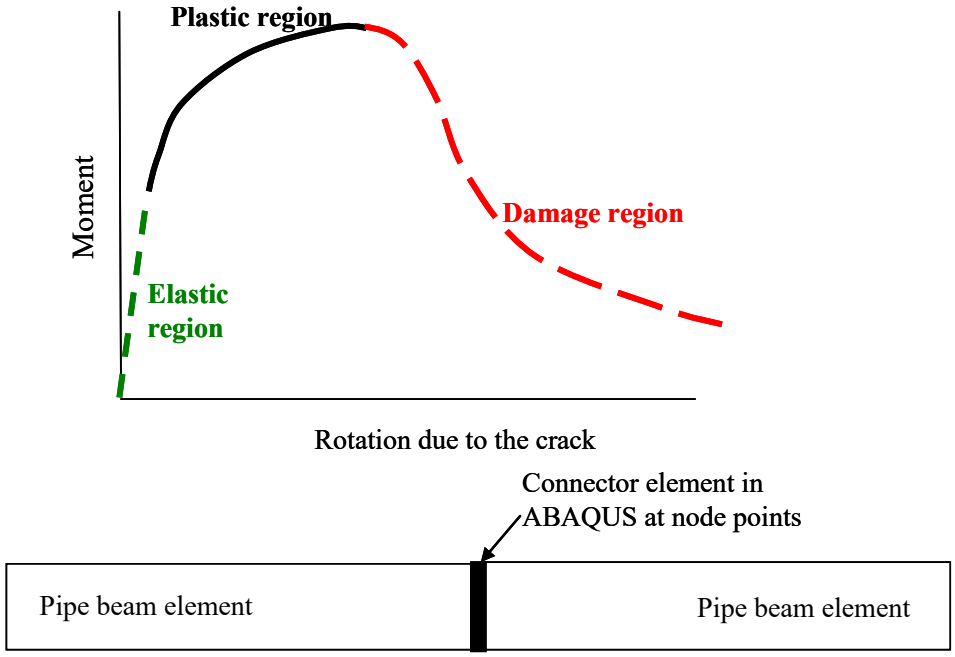

Figure 3-9 Simulation of a crack in current program using Abaqus

The “connector element” of Abaqus was used in this project to simulate the crack behavior, i.e., the moment versus rotation-due-to-the-crack response is modeled at a node point where the

crack is to be located. The “connector element” can be used to model complicated local behavior at a node point such as elastic behavior (linear and non-linear), plasticity (isotropic and kinematic type hardening), and damage (failure behavior until breakage occurs). In addition, this type of element can define admissible relative motion, which can be used to simulate the over-closure of a crack, i.e., when the crack faces come in contact under compressive loading, the pipe takes the compressive loads as if it were uncracked. Finally, damage can be introduced which includes the crack growth within the CPE. It should be noted that the use of this element is an improvement compared to the procedure used in past NRC/IPIRG programs using ANSYS where a series of springs and dashpots was required. Since this approach was a novel improvement to simplify the analyses, a thorough validation was conducted during its first implementation to understand the numerical behavior of the connector element before introducing it into the piping systems, see reference [9].

The use of the CPE is a huge computational advantage in that all the fracture mechanics evaluations are done outside of Abaqus, i.e., the connector element is tuned to the NRCPIPE/LBB.ENG2 J-estimation scheme. A nonlinear dynamic seismic analysis may need about 50,000 nonlinear FE analyses requiring very small time steps in order to converge and having a single element rather than 5,000 to 100,000 additional 3D elements to represent a crack is a huge CPU time savings. Additionally, if the 3D FE model is used, it would not include the crack growth – making the dynamic seismic analysis with crack-growth evaluations prohibitively time consuming.

As mentioned previously the local moment-rotation curve used in the connector element is nonlinear and comes from the LBB.ENG2 J-estimation scheme in the NRCPIPE code. Therefore, for each piping system several NRCPIPE runs are performed to determine the CPE input for each crack size.

It should be noted that the LBB.ENG2 J-estimation scheme works well for circumferential through-wall cracked pipe in bending. The method for combined pressure and bending assumed that the pressure is applied as an axial load like the pipe was endcapped. The assumption of the endcapped condition causes an induced additional bending. However, for a pipe system, that endcapped induced bending moment does not really exist. It is really the end nozzles that apply the bending, and they do not rotate more because of the pressure induced bending loads. The IPIRG pipe system tests showed that a full rupture of the pipe system with TWCs did not occur until the crack was ~95% of the circumference. That crack length corresponded to the net-section axial stress for the pressure loading reaching the material flow stress. Hence, for shorter cracks the combined pressure and bending solution in NRCPIPE was used, but for the longer crack cases, the pure bending solution was used, and the maximum moment was reduced to account for the axial stress on the net-section only (no induced bending) [17].

3.4.2 Effect of the Crack on the Piping System Integrity

As discussed in Section 2.2, the FE model of the piping system is run using only elastic properties when determining if the ASME Section III Code stress limits are met. Once it has

been determined that these limits are met, the plastic material properties are added to the model and the analysis is rerun. Simply introducing plasticity into the piping system has a significant impact on the peak applied moment for the same displacement-time history. The BWR RCIC system sees the peak applied moment drop from the uncracked elastic SL-D limit of 178,181 in-lb_f to 96,180 in-lb_f. For the PWR CVCS system driven at a loading frequency of 5 Hz, the peak applied moment drops from the uncracked elastic SL-D limit of 146,900 in-lb_f to 82,460 in-lb_f. The 3 Hz loading was closest to the uncracked pipe natural frequency of 2.91 Hz but had the lowest nonlinear moment with no crack for the same condition of reaching 3Sm in the elastic uncracked pipe dynamic loading used for all frequency loading. The other frequencies would have higher SAM loading which might explain this trend.

As the crack size is increased in the PWR CVCS system the peak applied moment continues to decline as shown in Figure 3-10, especially as the initial crack length in the CPE is increased.

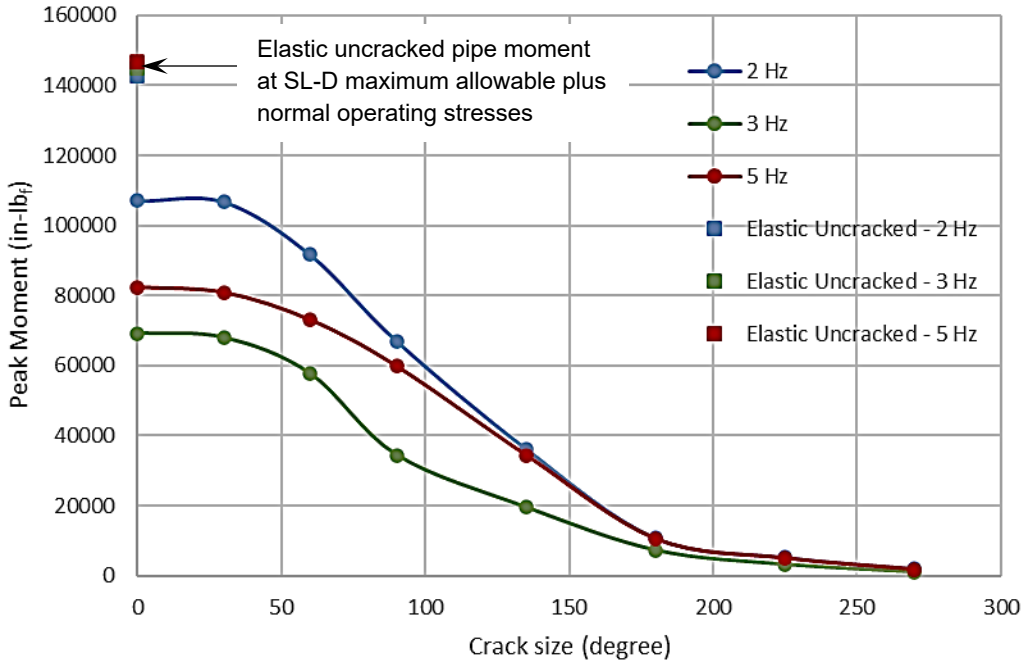

Figure 3-10 Peak moment as a function of crack size for the PWR CVCS system at different applied frequencies (uncracked pipe natural frequency was 2.91 Hz)

This trend is also seen in the BWR RCIC system where the peak applied moment decreases as the crack size increases as shown in Figure 3-11.

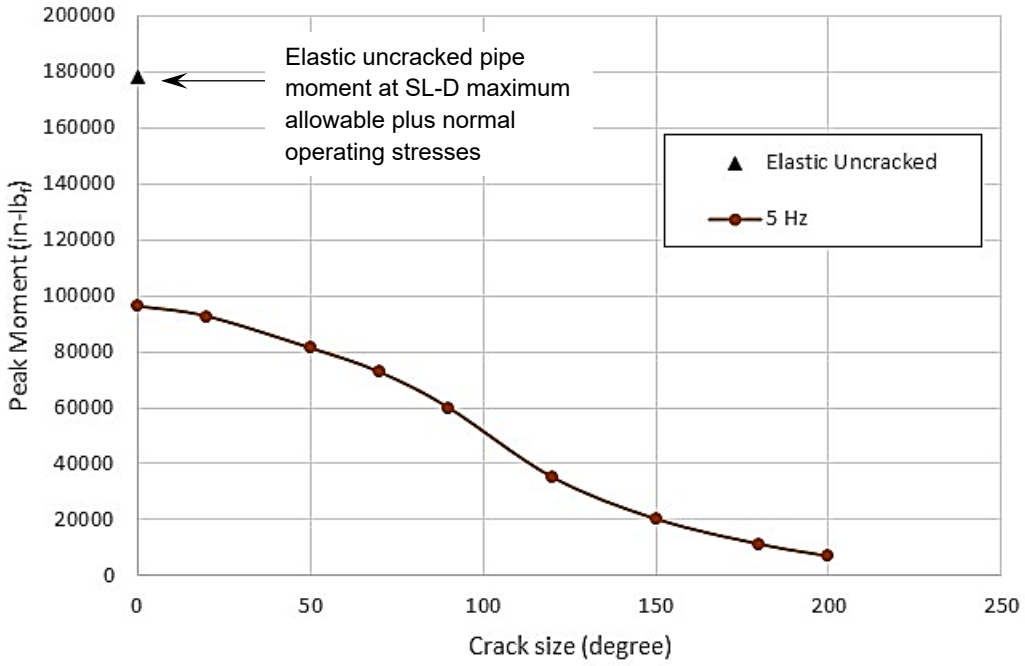

Figure 3-11 Peak moment as a function of crack size for the BWR RCIC system

The decrease in moment as a function of crack size shows that the piping system is acting more like it is under displacement-controlled loading rather than load-controlled loading. Under load-control, the peak moment would stay constant and should be independent of the crack size, which is an assumption in traditional LBB analyses in SRP 3.6.3 as well as in probabilistic analyses such as in xLPR. However, there is a clear, significant decline in the peak moment due to both plasticity and increasing crack size when compared to the uncracked linear-elastic peak moment. Typical LBB analysis assumes that the piping system is load-controlled for stability analysis and that the uncracked stresses are maintained when a crack is present. Both of these assumptions lead to significant over-conservatism in the estimation of the critical crack size.

The PWR CVCS pipe system has a natural frequency of 2.91 Hz as shown in Figure 3-3. When the elastic modal analysis is rerun with the presence of a crack, it is noted that the natural frequency decreased due to the compliance changes in conjunction with the local plasticity induced by the crack. Therefore, the natural frequency was determined over a range of crack sizes to ascertain the impact of the crack size. The results are shown in Figure 3-12. When there is a crack that is 180° around the circumference of the pipe that natural frequency drops to almost half the original value. The lowest applied frequency used was 2 Hz, which is closest to this minimum plateau frequency for long crack lengths.

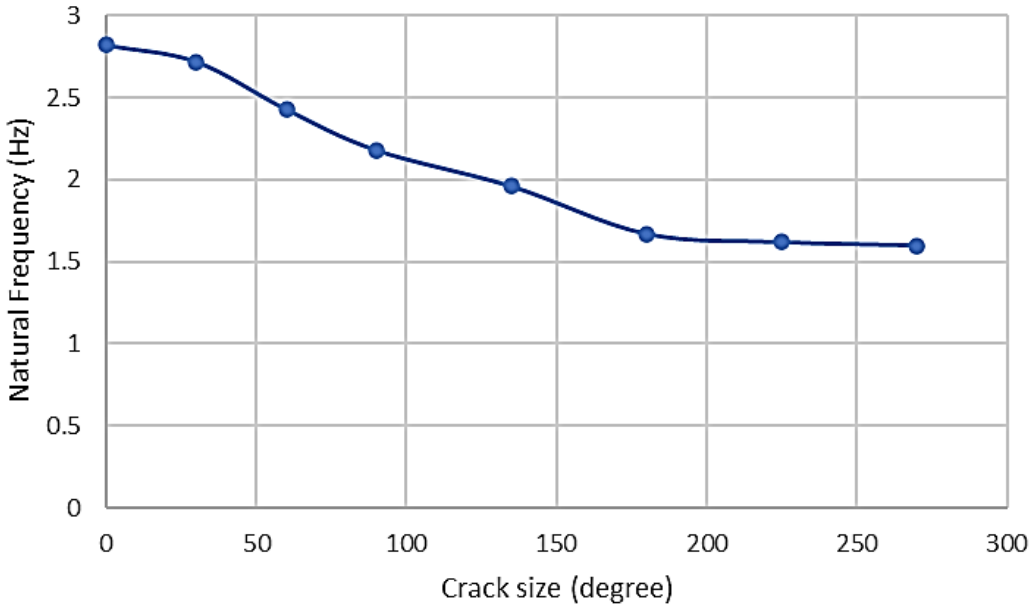

Figure 3-12 Natural frequency as a function of crack size for the PWR CVCS pipe system

3.4.3 Crack Stability Under Dynamic Loading

3.4.3.1 Critical Crack Size by SRP 3.6.3 Procedure

The maximum allowable inertial loading by Section III for SL-D is $3S_m$ for a pipe system that has a single-hinge point (not a well-balanced system). For the problem undertaken for this bounding evaluation, the S_m values used were 20 ksi even though the tensile test and fracture properties of TP304 and A106B at 550°F in the FE models were used. Hence $3S_m$ = 60 ksi.

By the ASME Section XI flaw evaluation procedure, the Net-Section-Collapse (NSC) analysis uses the flow stress of the material to determine the limiting flaw sizes. The Section XI procedures are for a surface flaw, where the same equations for a TWC are used in SRP 3.6.3. Flow stress is taken as the average of yield and ultimate strength at temperature. For TP304 at 550°F the flow stress is 41.15 ksi. For A106B at 550°F the flow stress is 43.825 ksi.

For the NSC equation given in Section XI, Appendix C, Paragraph C-5321, and consistent with SRP 3.6.3 guidance, the limiting case for no crack gives the elastic bending stress as $4*S_{flow}/\pi$. This gives the maximum elastic bending stress for piping without a crack as being 52.4 ksi for TP304 and 55.8 ksi for A106B.

The limit of the SL-D elastic stresses of 60 ksi that was applied for both cases in the dynamic analysis already exceeds the Section XI NSC maximum bending stress. This means that no circumferential flaw size could satisfy an SRP 3.6.3 LBB evaluation.

Adding in the normal operating stresses and SAM stresses to the SL-D inertial stresses would result in a bigger failure of LBB by SRP 3.6.3 traditional analyses.

3.4.3.2 Critical Crack Sizes from Advanced LBB Analyses

As was shown in Figure 3-10 and Figure 3-11, the peak applied moments in the cracked-pipe FE dynamic analysis dropped as the crack length was increased. This is consistent with all prior Emc^2 analyses for other pipe systems with circumferential TWCs. The following results illustrate crack stability.

Figure 3-13 shows the typical results of the applied moment versus rotation-due-to-the-crack from the inertial SL-D limiting moment with the normal operating stresses for the PWR CVCS pipe system. The input of the Abaqus connector element to represent the CPE, which is the LBB.ENG2 J-estimation procedure, is also shown as the red curve. The LBB.ENG2 moment-rotation due to the crack curve should be the upper-bound to the CPE, although Abaqus output is conservatively always a little under the response curve. The response curve represents the moment versus rotation strength curve for the cracked pipe. If the loading was sufficient to completely break the pipe, then the applied curve would follow the CPE moment-rotation bounding curve to the end on the input rotation, which represents the crack growing completely around the pipe circumference. As can be seen in these four different crack length analyses, the applied rotation is getting almost to the maximum moment, but there are huge margins on getting the applied rotation to the maximum rotation needed to cause a complete severance of the pipe. Hence there might be some small ductile tearing, but even maximum moment was not completely reached. Thus the crack could be even larger than 270-degrees before a complete severance might occur. From past IPIRG pipe system testing experience, the pressure loads would pull the pipe apart for a complete severance or rupture once the TWC in a pipe system was greater than 95-percent of the circumference.

Many additional crack length cases were run for both the PWR CVCS pipe system and BWR RCIC system cases, but they all resulted in the cracks being stable by the end of the loading history.

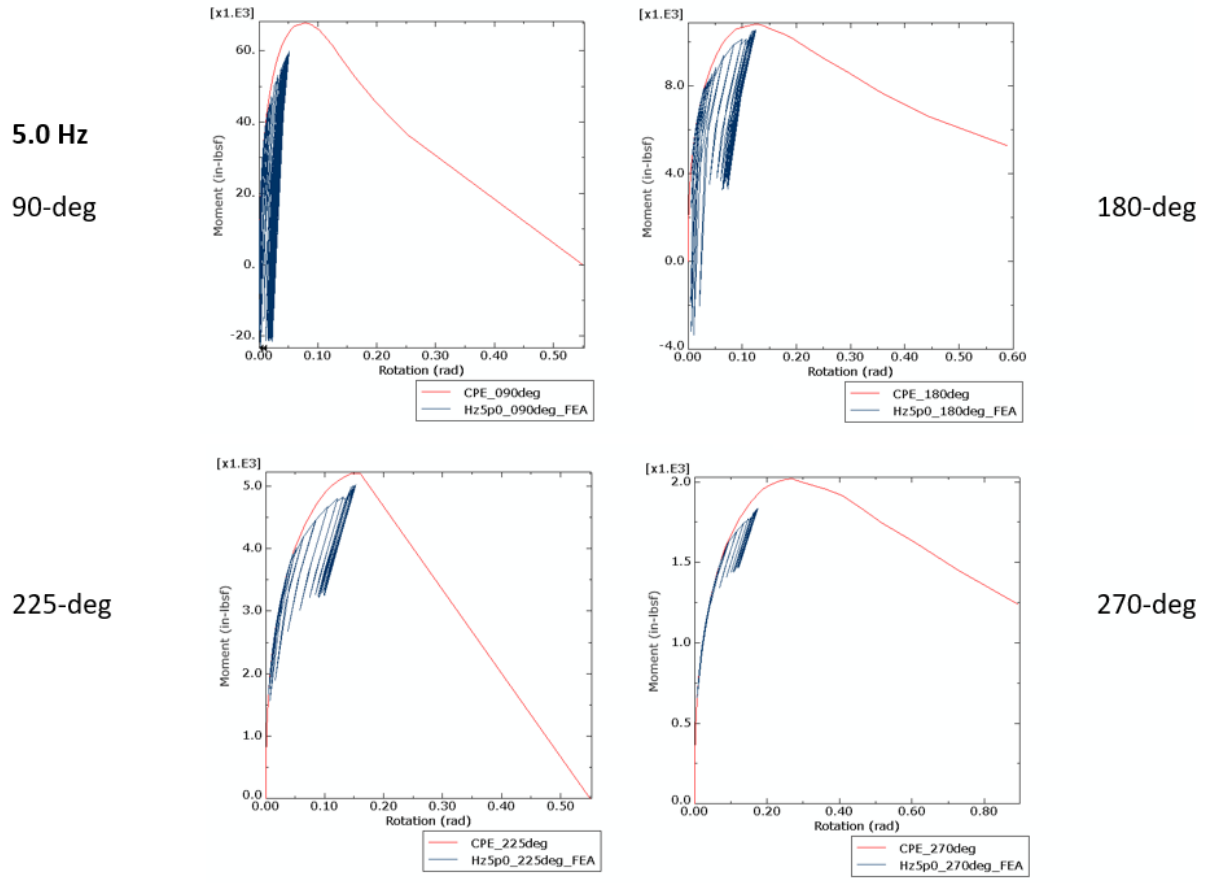

Figure 3-13 Applied moment versus rotation-due-to-the-crack for 4 different crack length cases using the PWR CVCS pipe system with the 5.0 Hz inertial loading at the SL-D maximum elastic stress limit plus the normal operating stresses.

3.4.4 Time Phasing of the SAM and Inertial Stresses

The SAM stresses were calculated from the dynamic analyses using the maximum endpoint/anchor motion displacements in a static analysis to ensure they were within the $6S_m$ limit of Section III NB-3656 SL-D loading. This has been done in some LBB submittals, while most other past LBB submittals did not indicate the SAM stresses. In typical response-spectrum dynamic design analyses, only the inertial stresses are calculated; hence estimates of the SAM are only made for Code allowable comparisons.

In the FE time-history analyses conducted in this project, the inertial and SAM contributions are combined in the dynamic moment output. In the uncracked-pipe analyses for the applied frequencies near the 1st natural frequency of 2.91 Hz, the peak moment versus time was completely out-of-phase with the applied end-displacement time history. Hence the displacements to produce SAM stresses are completely out-of-phase with the dynamic moments and the moments should primarily be inertial only, see Figure 3-14. However, at 2 Hz, the moments and displacement functions are in-phase, so there is some SAM contribution to

the total dynamic moment calculated by Abaqus, see Figure 3-15. The SAM contributions are far less than the $6S_m$ Code limit for SL-D loading.

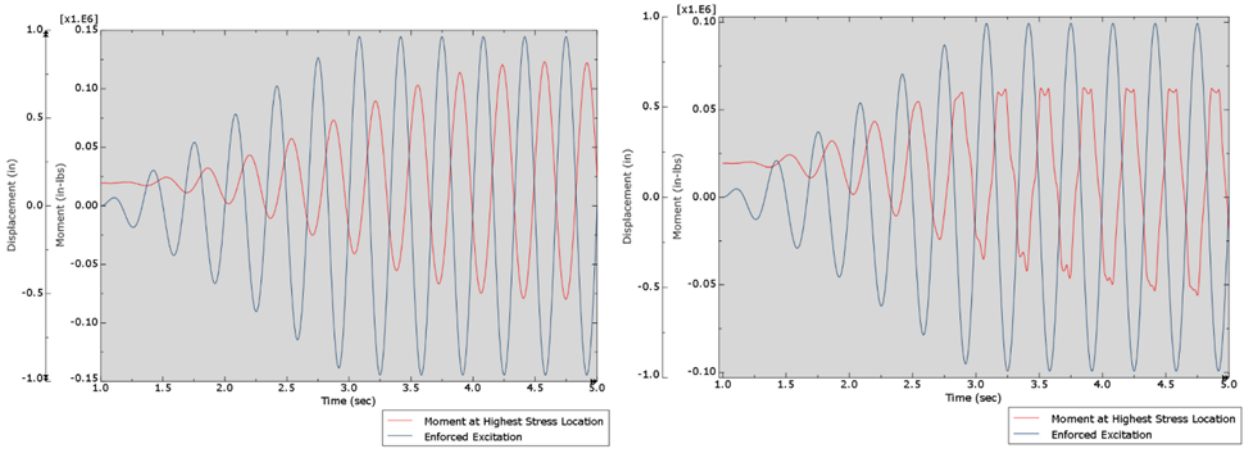

(a) Elastic uncracked (b) Nonlinear uncracked

Figure 3-14 Dynamic calculation for the PWR CVCS pipe system for highest stressed location at applied frequency of 3 Hz close to the natural frequency of 2.91 Hz

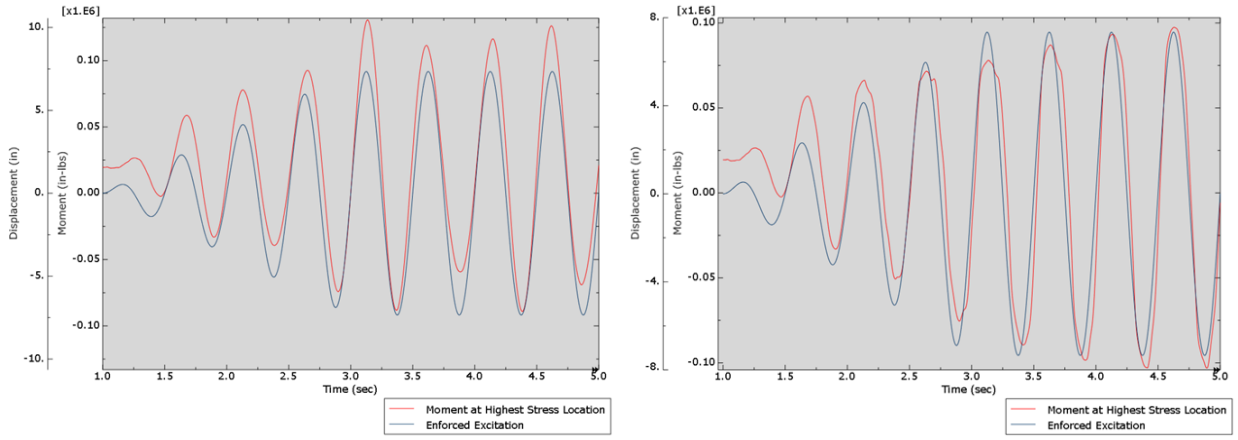

(a) Elastic uncracked (b) Nonlinear uncracked

Figure 3-15 Dynamic calculation for the PWR CVCS pipe system for highest stressed location at applied frequency of 2 Hz, below 1st natural frequency of 2.91 Hz

4 SUMMARY AND FURTHER WORK

4.1 Summary

The analysis performed to date examined an alternative way to assess the continued operation of smaller diameter high-energy/safety related piping rather than using the current SRP 3.6.2 and BTP 3-4 CUF approaches that came from 1970 methods. These smaller diameter systems that use the CUF approach find it more difficult to satisfy that criterion for plant life extension. The SRP 3.6.3 for LBB would be an alternative to using SRP 3.6.2 and BTP 3-4. Within the last decade it has been shown that the SRP 3.6.3 LBB approach has significant conservative assumptions, which make satisfying LBB difficult for small diameter piping. Those assumptions are eliminated by using the Robust LBB approach in this report, using more sophisticated FE analyses to incorporate the effects of the crack presence on the applied moments, as well as for incorporating nonlinear behavior due to crack plane and global piping plasticity.

The analyses conducted to date used pipe system geometries from typical BWR (RCIC) and PWR (CVCS) systems that were more likely to have unstable behavior due to dead-weight loading and configuration conditions that result in higher inertial loading. Additionally, lower bounding stress-strain curve and fracture toughness values at 550°F were used for the A106B and TP304 pipe systems, which is higher than actual operating temperatures for these systems. In addition, to bound other potential systems, maximum SL-D stresses were used rather than the actual lower seismic stresses.

The analyses conducted here used the normal operating stresses, maximum inertial SL-D loading and any SAM stresses that naturally occur from the dynamic time-history loading. With the elastic calculated stresses at this level, these systems would not pass SRP 3.6.3 LBB criteria (or any flaw size by ASME Section XI Appendix C criteria). However, when conducting the nonlinear FE analysis with the presence of the crack in the BWR RCIC and PWR CVCS pipe systems examined here with the same dynamic displacement-time history, all circumferential TWC cases (up to 270-degree circumferential TWCs) were stable.

These results are certainly encouraging that the realistic “critical” circumferential through-wall flaw lengths are greater than 75-percent of the pipe circumference. Such long circumferential through-wall flaws certainly would be caught by leakage detection even with the crudest of methods well before reaching the critical flaw size.

4.2 Further Work

Additional sensitivity studies can be performed to account for different operating conditions, such as higher operating temperature for the normal operating thermal expansion stresses, or different boundary conditions to impart the maximum allowed dead-weight stresses. As discussed in the piping-system selection, low toughness and high inertial loading often lead to difficulty in achieving realistic LBB behavior. Therefore, sensitivity studies that evaluate the effect of different material properties or higher dead-weight loading in combination with the

inertial loading could lead to useful information to provide guidelines or a screening criterion for changes to SRP 3.6.2 or BTP 3-4.

However, the “critical” flaw size evaluation in this work to date, assumes that there will be a relatively short length TWC developing and growing rather than a potential 360-degree surface crack that might rupture without any leakage warning. This crack-shape development aspect still needs to be addressed and may be the next most important sensitivity study to conduct.

An encouraging aspect is that for thinner-walled piping, there are not many weld beads in the weldment compared to primary loop piping. From other work done for refinery piping [10], the transient weld start-stop locations have been found to produce weld residual stresses that are tensile completely through the thickness. These locations have been found to be precursor leakage locations in refinery piping, see Figure 4-1 and Figure 4-2. These field observations confirmed FE weld simulation analyses and the FE simulations of small-diameter nuclear piping girth welds should likewise show that the start/stop locations of the welding tend to promote LBB in thin-walled piping typical of these pipe diameters.

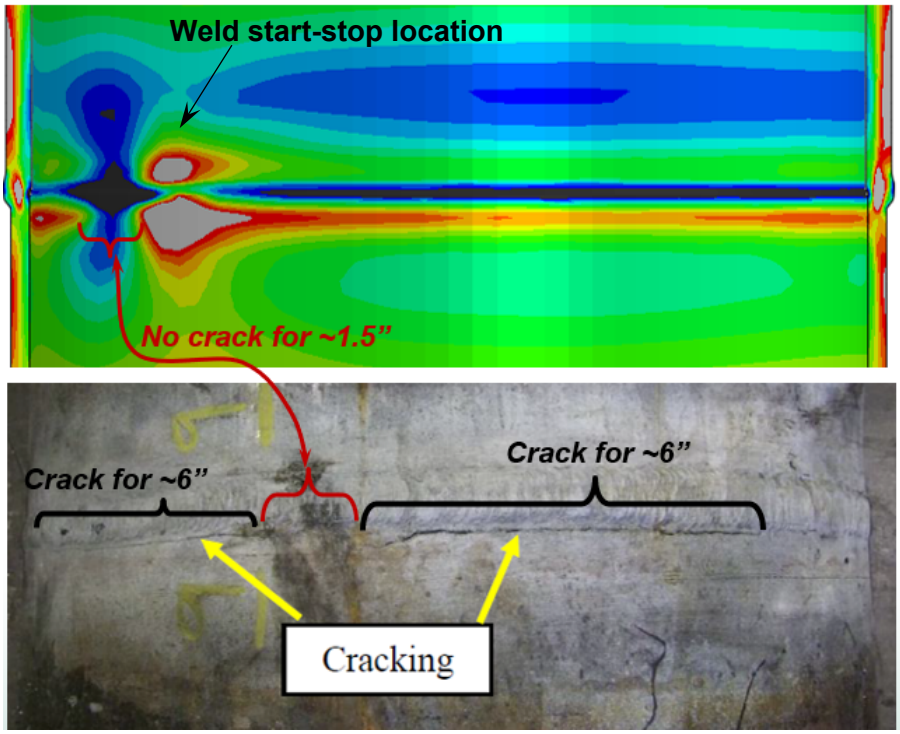

Figure 4-1 Illustration of transient weld residual stress analysis showing the high tensile stresses at a welding start-stop location, and the crack observed in service for a refinery piping system

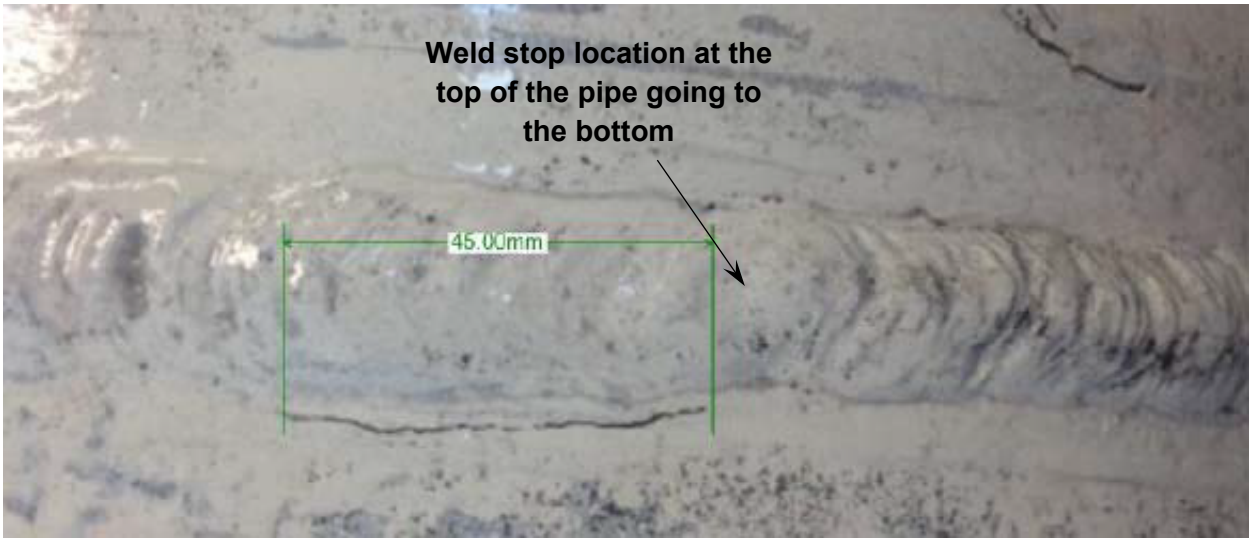

Figure 4-2 Example of a crack starting at the top of a pipe where the weld was made in the downhill welding position from the top to the bottom along both sides of the pipe (typically two welders make this weld at the same time on opposite sides of the pipe)

To gain additional confidence, there should be some leakage calculations at normal operating conditions for different crack lengths. A bounding crack growth analysis (i.e., conservative SCC rate or fatigue crack growth rate) could be used to conservatively estimate the leak rate and cumulative leakage with time. Margins on the leakage detection capabilities at these pipe-system locations would be established to give comfort to the criterion and the needs for repair/replacement scheduling. Such analyses were previously conducted for the Atucha II NPP in Argentina [9]. This fatigue crack growth rate calculation for the intent of identifying detectable leakage versus time, is quite different than the CUF S-N based fatigue analysis originally in SRP 3.6.2 and BTP 3-4.

These sensitivity studies along with the work described in this report would provide a technical basis for developing alternative acceptance criteria to the current BTP 3-4 guidance.

5 REFERENCES

[1] NRC, "Modification of General Design Criterion 4 Requirements for Protection Against Dynamic Effects of Postulated Pipe Ruptures," *Federal Register,* pp. 27,006-27,009, 1 July 1985.

[2] NUREG-0800 Chapter 3 - Section 3.6.3, "Leak-Before-Break Evaluation Procedures," U.S. Nuclear Regulatory Commission, 2007.

[3] NUREG-0800 Chapter 3 - Section 3.6.2, "Determination Of Rupture Locations and Dynamic Effects Associated with the Postulated Rupture of Piping," U.S. Nuclear Regulatory Commission, 2015.

[4] NRC Branch Technical Position 3-4, "Postulated Rupture Locations in Fluid System Piping Inside and Outside Containment," ML070800008, 2007.

[5] NRC Branch Technical Position 3-3, "Protection Against Postulated Piping Failures in Fluid Systems Outside Containment," ML070800027, 2007.

[6] NRC NUREG-1800 Rev 2, "Standard Review Plan for Review of License Renewal Applications for Nuclear Power Plants," ML103490036, 2010.

[7] NRC NUREG-2192, "Standard Review Plan for Review of Subsequent License Renewal Applications for Nuclear Power Plants," ML17188A158, 2017.

[8] A. Hopper, G. Wilkowski , P. Scott and R. Olson, "NUREG/CR-6452, The Second International Piping Integrity Research Group (IPIRG-2) program. Final report," U.S. Nuclear Regulatory Commission, 1997.

[9] G. Wilkowski, B. Brust, T. Zhang, G. Hattery, S. Kalyanam, D.-J. Shim, E. Kurth, Y. Hioe, M. Uddin, J. Johnson, P. Asfura, A. A. Betervide and O. Mazzantini, "Robust LBB Analyses for Atucha II Nuclear Plant, PVP2011-57939," in *ASME PVP Conference*, 2011.

[10] G. Wilkowski, Y. Hioe, E. Kurth, E. Punch, M. Uddin, F. Brust, K. Bagnoli and G. Pioszak, "Initial Developments for LBB Application to HTHA Sensitive Non-stress RElieved Carbon Steel Girth Welds in Refinery Plants, PVP2018-84669," in *ASME PVP Conference*, Prague, Czech, 2018.

[11] G. M. Wilkowski and e. al, "Degraded Piping Program - Phase II - Summary of Technical Results and Their Significance to Leak-Before-Break and In-Service Flaw Acceptance Criteria, NUREG/CR-4082 Volume 8," March 1989.

[12] ASME, "Boiler and Pressure Vessel Code Section III, Division 1, Subsection NB," 2019 Edition.

[13] ASME, "Boiler and Pressure Vessel Code, Section II, Part D," 2019 Edition.

[14] U.S. Nuclear Regulatory Commission Office of Nuclear Regulatory Research, "Regulatory Guide 1.6, Design Response Spectra for Seismic Design of Nuclear Power Plants, Rev 2," July 2014.

[15] R. Olson, R. Wolterman, P. Scott, P. Krishnaswamy and G. Wilkowski, "The Next Generation Methodology for Cracked Pipe System Subjected to Dynamic Loads," *ASME PVP,* vol. Vol 275, no. 1, pp. 159-172, June 1994.

[16] R. J. Olson, R. L. Wolterman, G. M. Wilkowski and C. A. Kot, "Validation of Analysis Methods for Assessing Flawed Piping Subjected to Dynamic Loading," NUREG/CR-6234, August 1994.

[17] S. Kalyanam, G. Wilkowski, S. Pothana, Y. Hioe, C. Sallaberry and J. Martin, "Apparent Net-Section-Collapse Methodology for Circumferential Surfacde Flaws in Piping," in *Proceedings of the ASME 2017 Pressure Vessels & Piping Conference, PVP2017-65438*, July 16-20, 2017.

IMPENDING PUBLICATION OF TECHNICAL LETTER REPORT ENTITLED “TECHNICAL SUPPORT FOR COMPONENT INTEGRITY - POSTULATED PIPE RUPTURE LOCATIONS” (TLR-RES/DE/REB-2022-09) DATE October 5, 2022

DISTRIBUTION:
RIyengar, RES/DE/CIB
SBailey, R-II/DRP/RPB4
KManoly, NRR/DEX
CBasavaraju, NRR/DEX/EMIB
DRudland, NRR/DNRL
RTregoning, RES/DE
NChandran, RES/DE/REB

ADAMS Accession No.: ML22277A503; ML22277A504

OFFICE	RES/DE/CIB	RES/DE/CIB	RES/DE	
NAME	BLin *BL*	RIyengar *RI*	LLund *LL*	
DATE	Oct 4, 2022	Oct 4, 2022	Oct 5, 2022	

OFFICIAL RECORD COPY